Visual Neuroscience (2003), **20**, 663–686. Printed in the USA.

DOI: 10.1017/S0952523803206088

Complete flatmounting of the macaque cerebral cortex

LAWRENCE C. SINCICH, DANIEL L. ADAMS, AND JONATHAN C. HORTON
Beckman Vision Center, University of California—San Francisco, San Francisco

(RECEIVED October 21, 2003; ACCEPTED October 28, 2003)

Abstract

The elaborate folding of the brain surface has posed a practical impediment to investigators engaged in mapping the areas of the cerebral cortex. This obstacle has been overcome partially by the development of methods to erase the sulci and gyri by physically flattening the cortex prior to sectioning. In this study, we have prepared a step-by-step atlas of the flatmounting process for the entire cerebral cortex in the macaque monkey. The cortex was dissected from the white matter, unfolded, and flattened in a single piece of tissue by making three relieving cuts. The flatmount was sectioned at 60–75 μm and processed for cytochrome oxidase (CO) or myelin. From animal to animal there was nearly a twofold variation in the surface area of individual cortical regions, and of the whole cortex. In each specimen, a close correlation was found between V1 surface area (mean = 1343 mm^2), V2 surface area (mean = 1012 mm^2), hippocampal area (mean = 181 mm^2), and total cerebral cortex area (mean = 10,430 mm^2). The complete pattern of CO stripes in area V2 was labeled clearly in several cases; the number of cycles of thick-pale-thin-pale stripes ranged from 26 to 34. Characteristic patterns of strong CO activity were encountered in areas V3, MT, auditory and somatosensory cortex. In some animals we made injections of a retrograde tracer, gold-conjugated cholera toxin B subunit, into area V2 to identify all sources of cortical input. In addition to previously described inputs, we identified three new regions in the occipitotemporal region that project to V2. Flatmounting the cerebral cortex is a simple, efficient method that can be used routinely for mapping areas and connections in the macaque brain, the most widely used primate model of the human brain.

Keywords: Cortical areal measurements, Brain unfolding, Computer flattening, V2 projections

Introduction

The challenge of identifying distinct anatomical areas within the cerebral cortex of the primate brain has beckoned neuroanatomists for more than a century. The traditional approach, exemplified by Brodmann's (1909) famous cytoarchitectonic atlas, has relied on analysis of serial cross sections of the intact brain cut in either the coronal, sagittal, or horizontal plane. The borders between different areas can be recognized, in principle, by noting transitions in the density, type, and laminar arrangement of cells and processes stained with various histological techniques.

Some architectonic divisions and patterns, however, are more evident in tissue sections cut parallel to the pial surface. The barrel field in rodent somatosensory cortex furnishes a prime example. Numerous classical anatomists observed cell columns in cross sections of layer 4, but missed entirely their significance (De Vries, 1912; Rose, 1912; Droogleever Fortuyn, 1914; Lorente De Nó, 1922). It was not until Woolsey and Van Der Loos (1970) cut the cortex in tangential section that the barrel field leapt into view. Moreover, upon seeing its pattern in two dimensions, Woolsey and Van Der Loos knew instantly and intuitively that the larger barrel field corresponded to the mystacial vibrissae.

The description of the rodent barrel field provided the impetus for the birth of the cortical flatmount technique. To capture the barrel field in just a few tangential sections, Welker and Woolsey (1974) removed parts of the basal forebrain to relax the brain surface. The cortex then was flattened artificially by compressing it between two glass slides during fixation and embedding. Welker and Woolsey noted "this to be a particularly useful innovation" because it yielded large tangential sections of the highly convex rodent hemisphere.

The flatmount technique was later used to flatten the exposed opercular surface of macaque striate cortex prior to sectioning for deoxyglucose autoradiography (Tootell et al., 1982). It was also used to survey the pattern formed by cytochrome oxidase (CO) patches throughout striate cortex (Horton, 1984). Cuts were made along the crests of gyri and the depths of sulci. The resulting fragments, each relatively flat, were then frozen individually against glass slides. This permitted tangential sectioning of the entire striate cortex, including regions buried within the calcarine fissure.

A breakthrough occurred in 1985 when a technique was developed for unfolding the gyri of the cortex prior to flatmounting (Olavarria & Van Sluyters, 1985; Tootell & Silverman, 1985). This method allowed flatmounting of vast expanses of cortex, while preserving an intact sheet of tissue. Subsequently, complete flat-

Address correspondence and reprint requests to: Jonathan C. Horton, Beckman Vision Center, University of California—San Francisco, 10 Koret Way, San Francisco, CA 94143-0730, USA. E-mail: horton@itsa.ucsf.edu

mounts have been prepared of the cerebral cortex in the cat (Olavarria & Van Sluyters, 1985), owl monkey (Tootell et al., 1985; Krubitzer & Kaas, 1993; Beck & Kaas, 1998), slow loris (Preuss et al., 1993), marmoset (Krubitzer & Kaas, 1993; Lyon & Kaas, 2001), galago (Krubitzer & Kaas, 1993; Collins et al., 2001), and squirrel monkey (Beck & Kaas, 1998). In the macaque, large portions of the cerebral cortex have been flatmounted (Felleman et al., 1997; Beck & Kaas, 1999; Lyon & Kaas, 2002). However, no laboratory has succeeded at flatmounting the entire macaque cortex, because of its large size and extensive convolutions. Here, we describe complete flatmounting of the macaque cerebral cortex and apply this technique in conjunction with histochemistry, myelin staining, and retrograde tracing to map the cortical connections of area V2.

Materials and methods

Experimental animals and procedures

Ten fully adult macaque monkeys (three *Macaca mulatta* and seven *Macaca fascicularis*), were used in this study (Table 1). All but one were male. In most cases the animals were used in connection with other projects, and consequently only one hemisphere was available for flatmounting. All procedures followed a protocol approved by the Committee on Animal Research at the University of California, San Francisco.

In two animals, tracer injections were made of ~140 nl of 0.1% gold-conjugated cholera toxin B subunit (CTB) (List Biological Laboratories, Campbell, CA) spaced 5.5 mm apart in V2 along the posterior lip of the lunate sulcus at a depth of 600 μm (Sincich & Horton, 2002*a*). Anesthesia was induced with ketamine HCl (15 mg/kg i.m.). The animal was intubated and respirated with 1–1.5% isoflurane in 1:1 N_2O:O_2. After a craniotomy the dura was opened to expose 35 mm of the lunate sulcus. CTB was pressure injected under direct visual guidance. Postoperatively, animals were treated with buprenorphine (0.02 mg/kg i.m.) every 8 h until fully recovered.

The flatmount technique

After 3–7 days for transport, animals were killed with pentobarbital (150 mg/kg) and perfused rapidly *via* the left ventricle with 1 l filtered 0.9% saline followed by 1 l 1% paraformaldehyde in 0.1 M phosphate buffer solution (PB), pH = 7.4. The brain was removed from the skull immediately after perfusion and placed in PB. Throughout the dissection, the brain was kept moist with buffer; drying of the tissue caused artifactual loss of CO activity. The best flatmounts were achieved when dissection began immediately after removing the brain from the skull; leaving it in solution for even a few hours made unfolding the tissue more difficult. Unperfused, unfixed cerebral cortex can also be flattened easily.

The flatmount process is illustrated step-by-step in Fig. 1, in the hope that it will be useful to other laboratories. For clarity, there are two sets of images showing the dissection sequence: (1) a series of near life-size photographs, unobscured by labels, of the dissection of the right hemisphere of Monkey 1; and (2) a companion set of diagrams with the sulci labeled and the relieving cuts marked to help the reader follow the topology of the hemisphere as it unfolds. After some practice, the dissection takes about 4–6 h per hemisphere. An 18-s movie, prepared by blending sequential photographs (Elastic Reality, Avid Technology, Tewksbury, MA), provides a time-lapse view of the flatmount procedure (available at www.ucsf.edu/hortonlab).

As the dissection proceeds, the tissue becomes a thin, fragile sheet. For ease of handling, it is placed on a 5 × 7 inch glass slide (Brain Research Labs, Newton, MA). The flatmount is inverted by placing it between two glass slides, and flipping the sandwich. The best dissection tools are wet cotton swabs, especially the smaller

Abbreviations

The names for sulci and gyri were based on designations provided by NeuroNames, University of Washington, at: http://rprcsgi.rprc.washington.edu/neuronames/index1.html.

Sulci

AS	Arcuate Sulcus
CF	Calcarine Fissure
CiS	Cingulate Sulcus
CS	Central Sulcus
ECS	Ectocalcarine Sulcus
FOS	Fronto-orbital Sulcus
IOS	Inferior Occipital Sulcus
IPS	Intraparietal Sulcus
LS	Lunate Sulcus
OTS	Occipitotemporal Sulcus
STS	Superior Temporal Sulcus
POM	Parieto-occipital Sulcus (medial)
POS	Parieto-occipital Sulcus
PS	Principal Sulcus
RS	Rhinal Sulcus
SF	Sylvian Fissure
SPCS	Superior Post-central Sulcus

Gyri

AG	Angular Gyrus
CG	Cuneate Gyrus
CiG	Cingulate Gyrus
FOG	Fronto-orbito Gyrus
FuG	Fusiform Gyrus
GR	Gyrus Rectus
IFG	Inferior Frontal Gyrus
IOG	Inferior Occipital Gyrus
ITG	Inferior Temporal Gyrus
LiG	Lingual Gyrus
MFG	Middle Frontal Gyrus
MOG	Medio-occipital Gyrus
MTG	Middle Temporal Gyrus
Oper	Operculum
PCG	Pre-cuneate Gyrus
PHG	Parahippocampal Gyrus
PrG	Precentral Gyrus
PoG	Postcentral Gyrus
SFG	Superior Frontal Gyrus
SMG	Supra-marginal Gyrus
SPL	Superior Parietal Lobule
STG	Superior Temporal Gyrus

Thalamic Structures

cc	corpus collosum
ox	optic chiasm
ac	anterior commissure
ic	internal capsule

Table 1. *Areal measurements in flatmount specimens*

Hemisphere	Animal weight (kg)	Total area (mm^2)										% Area of neocortex	
		Flatmount	V1	V2d	V2v	V2	MT	A1	S1	Hippocampus	Neocortex	V1	V2
Monkey 1L	9.0	9174	1106	441	413	854	38	96	183	185	8989	12.3	9.5
Monkey 1R		8867	1146	463	421	884	68	61	194	146	8721	13.1	10.1
Monkey 2R[a]	12.0	14,353	1774	671	741	1412	94	91	259	240	14,113	12.6	10.0
Monkey 3R	9.5	11,230	1485	476	455	931	88	99	265	181	11,049	13.4	8.4
Monkey 4R	2.8	10,386	1236	543	487	1030	66	75	319	216	10,170	12.2	10.1
Monkey 5R	7.4	8395	991	426	356	782	99	74	301	109	8286	12.0	9.4
Monkey 6R[a,b]	8.0	13,037	1817	453	712	1165	58	115	397	258	12,779	14.2	9.1
Monkey 7L	4.1	10,302	1356	536	524	1060	91	64	282	187	10,115	13.4	10.5
Monkey 8R	4.0	9297	1123	482	415	897	75	127	317	148	9149	12.3	9.8
Monkey 9R	8.4	11,070	1393	556	546	1102	54	82	323	144	10,926	12.7	10.1
Monkey 10R[a,c]	9.9	—	1950	—	—	—	—	—	—	—	—	—	—
Mean		10,611	1343	505	507	1012	73	88	284	181	10,430	12.8	9.7
SD		1897	281	74	129	185	20	21	63	47	1859		

[a]*Macaca mulatta*.
[b]Female.
[c]This animal not included in means because a complete flatmount was not prepared.

sizes, or calcium alginate swabs (Fisher Scientific catalogue # 14-960-3P and 14-959-77).

When the tissue is completely unfolded, it is postfixed under weight with the pial surface flattened against a glass slide (Fig. 2). A soft foam sponge is placed in an 11 × 7 inch glass dish (Pyrex # 232-R) and soaked in 1.5 % paraformaldehyde in PB plus 30% sucrose, taking care to eliminate any air bubbles. The sponge is covered with a sheet of filter paper to prevent formation of an imprint of the sponge pattern on the back of the flatmount. The cortex is placed (white matter down) on the filter paper and coaxed flat for a final time. A 5 × 7 inch slide is then carefully lowered onto the tissue, starting from one edge to insure that no air bubbles are trapped between the tissue and the slide. A beaker is placed on top, filled with sufficient water to achieve the desired flattening pressure (about 5 g/cm^2). The tissue is left overnight at 4°C for cryoprotection and additional fixation.

The next day, the flatmount (Fig. 3) is peeled off the glass slide and placed in a fresh solution of 1.5% paraformaldehyde plus 30% sucrose. If it sinks, it is cryoprotected for frozen sectioning. Modeling clay is built up around the edges of a freezing stage with a 5 × 6.5 inch surface (custom-built to this size by Brain Research Laboratories, Boston, MA). After dry ice powder is placed in the end troughs, the surface of the freezing stage is flooded with Tissue-Tek (#4583, Sakura Finetek, Torrance, CA). As soon as it freezes, forming a mesa ~ 5 mm high, the modeling clay walls are peeled away.

The dry ice is removed from the end troughs and about 50 randomly spaced holes are drilled 3–4 mm into the Tissue-Tek platform with a 2-mm burr on a Dremel drill. The Tissue-Tek is warmed by rubbing with the palm of the hand until the surface becomes slightly tacky. These steps are intended to promote adhesion of the specimen to the platform, so that it does not shear off during sectioning. A clean 5 × 7 inch slide is covered with Saran Wrap, leaving no wrinkles, and the flatmount is placed on it (white matter up). The slide is then flipped over and any air trapped between the flatmount pial surface and the glass slide is squeezed out using light fingertip pressure. A dollop of fresh Tissue-Tek is applied to the surface of the tacky (but still frozen) Tissue-Tek platform. The glass slide (with the specimen clinging to its underside) is immediately lowered into place. While the Tissue-Tek flows outwards under gentle pressure between the platform and specimen, an assistant rapidly dumps spoonfuls of dry ice powder onto the top of the glass slide. The entire flatmount freezes within 30–60 s. The dry ice is brushed off and the slide removed, leaving the film of Saran Wrap on the pial surface of the specimen. This is gently pulled off, yielding a perfectly flat surface for cutting.

It is crucial to leave no air pockets under the specimen, so ample liquid Tissue-Tek must be applied while mounting the specimen onto the frozen Tissue-Tek platform. Extra Tissue-Tek that appears around the flatmount edges during freezing should be trimmed away. This can be done with a Dremel drill or a razor blade. If Tissue-Tek is left along the leading edge of the specimen, score marks will appear on the sections. Dry ice with pure ethanol in the end troughs is used to keep the specimen frozen during sectioning. About 20 sections are cut at 60–75 μm with an AO-860 sliding microtome. They are mounted immediately from PB onto double-subbed (1.5% gelatin, 0.05% chrom alum) 5 × 7 inch slides. Usually, the first few sections are too fragmented to retain. Excess buffer is drained and the sections are dried at an angle to minimize solute precipitation. Sections are air-dried for ~ 24 h at room temperature and then reacted for CO activity (Horton, 1984) or stained for myelin with the Gallyas silver method (Gallyas, 1979). The CO sections are digitally imaged (to document CO patterns, before they are obscured by CTB processing) and then silver-intensified with an IntenSE-M silver intensification kit (Amersham Pharmacia, Piscataway, NJ) to reveal CTB label (Llewellyn-Smith et al., 1990; Boyd & Casagrande, 1999).

Data analysis

Whole flatmount sections were digitized at 400 dpi using a flatbed scanner with a transparency adapter. They were imported into Photoshop 6.0 or Illustrator 9.0 (Adobe Systems, San Jose, CA) to generate figures. Measurements were made from the scanned images using CADtools 2.1, an Illustrator plug-in (Hot Door, Inc., Grass Valley, CA). The total hemispheric areas were measured from digital photographs of the final tissue flatmounts before they were sectioned. Measurements of different functional areas and patterns were made from borders drawn onto scanned images of the CO- or Gallyas-stained sections. In some instances, regions

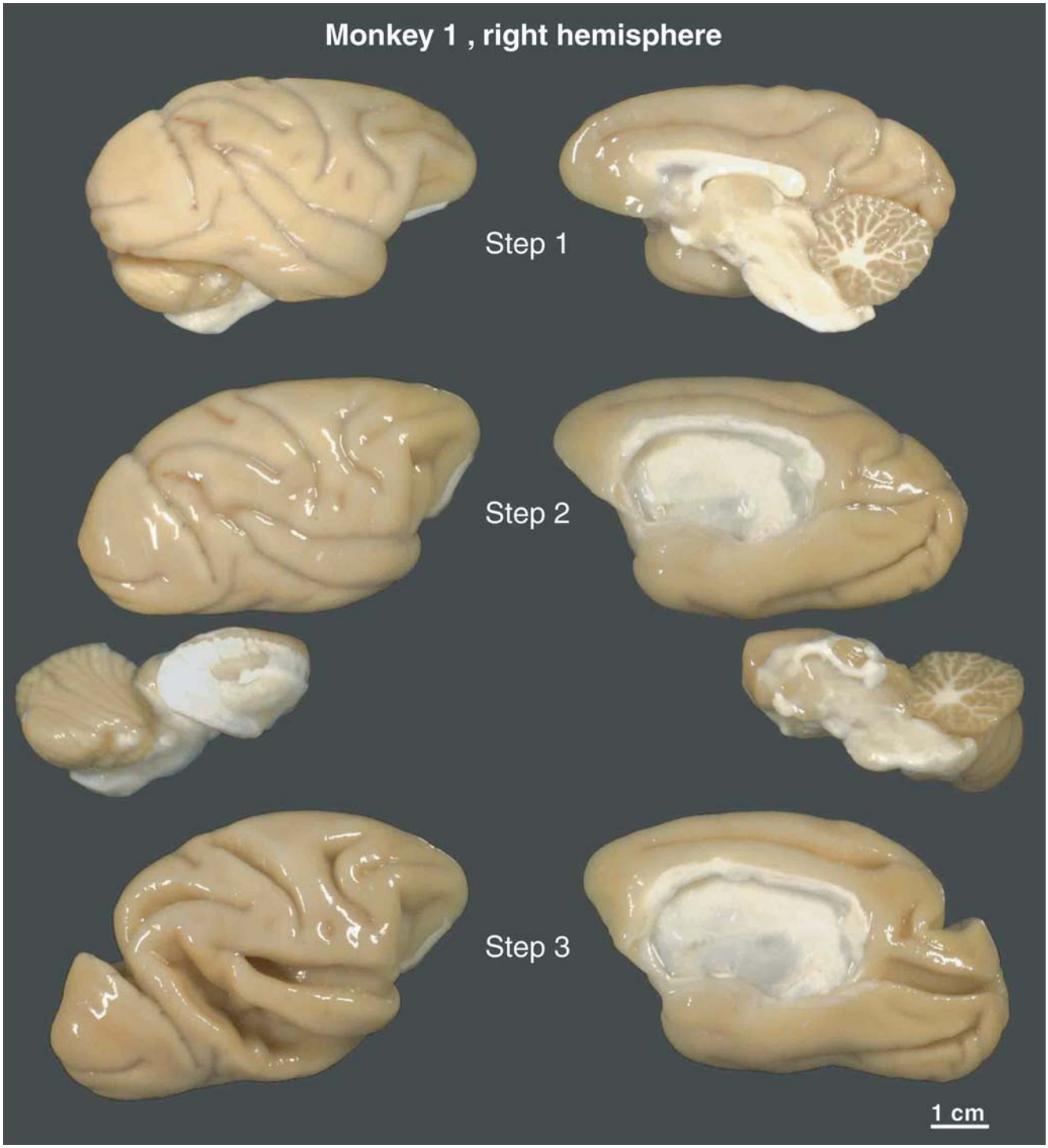

Fig. 1. Part 1. Monkey 1. *Step 1*: Using fingers, the brain hemispheres are gently pried apart and bisected along the midline with a scalpel. *Step 2:* A cotton swab moistened with PB is used to open a dissection plane in the corpus callosum (dashed line in *Step 1* diagram, Medial view), using a combination of stroking and swirling motions. This plane is followed laterally until the thalamus starts to separate from the cortex. Jeweler's forceps are used to peel away the pia-arachnoid membranes connecting the temporal lobe and the ventral thalamus. A cotton swab is inserted into the white matter, between the parahippocampal gyrus and the optic tract, to open another dissection plane that is followed laterally, to connect with that originating from the corpus callosum. At this point, the cortex is nearly loose, except for a gray matter connection just below the genu of the corpus collosum at the gyrus rectus (**, *Step 1* diagram, Medial view). This is cut, freeing the cerebral cortex from the rest of the brain.

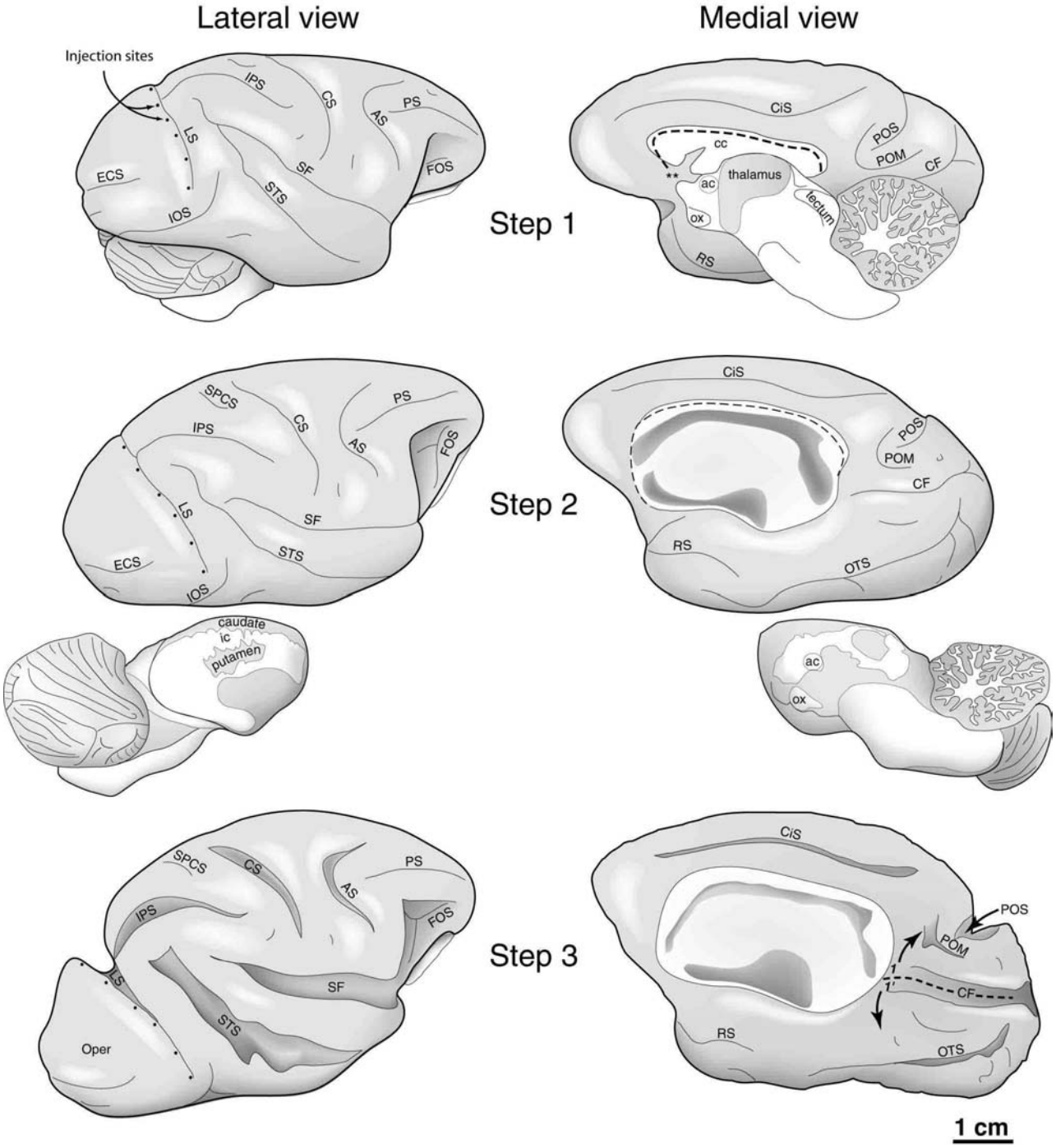

Fig. 1 continued. Part 1 continued. *Step 3, Lateral view*: Surface blood vessels are removed with fine forceps. A cotton swab is gently insinuated into the base of each sulcus, breaking all arachnoid adhesions. *Step 3, Medial view:* A subcortical dissection plane is opened, starting from the remnants of the splenium of the corpus callosum and extending posteriorly along the calcarine fissure to the occipital pole. The first relieving cut (dashed line) is started along the base of the calcarine fissure, from (*1,1'*) to a point just short of the occipital pole.

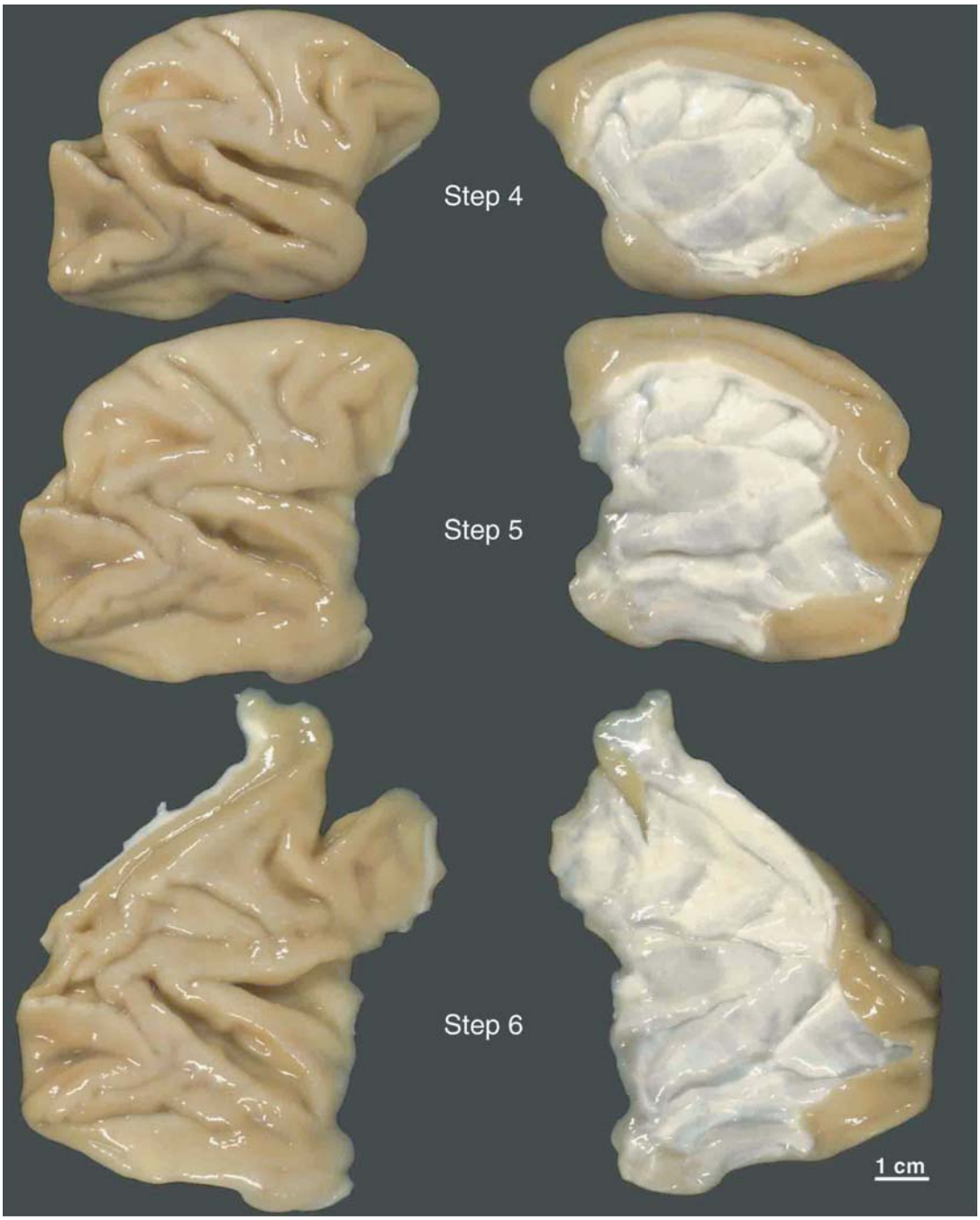

Fig. 1 continued. Part 2. *Step 4*: Dissection is extended under the banks of the calcarine fissure (curved arrows) to relax the cortex further. The second relieving cut is started at the gyrus rectus (*2,2'*), allowing the hippocampal region to unroll (curved arrow). *Step 5, Medial view*: A swab is inserted under the free edge of the cingulate gyrus and a dissection plane carried dorsally, underneath the cingulate sulcus (CiS), as far as possible. The second relieving cut is continued from (*3,3'*) along the frontal pole of the hemisphere (heavy dashed line). This permits the flap of anterior cingulate cortex to swing open (curved arrow).

were photographed at higher power using a SPOT RT digital camera (Diagnostic Instruments, Sterling Heights, MI) attached to an Olympus SZH10 microscope.

The distribution of CTB-labeled cells was plotted at 100× using a Zeiss Axioskop microscope. A grid of 2 × 2 mm squares (80 rows × 50 columns) was placed onto the glass slide to keep track of the location of labeled cells in the flatmount. This was done by printing the grid pattern, comprised of fine dotted lines, on a piece of paper using a laserjet printer. The underside of the glass slide was wetted with xylene and the paper was pressed against it.

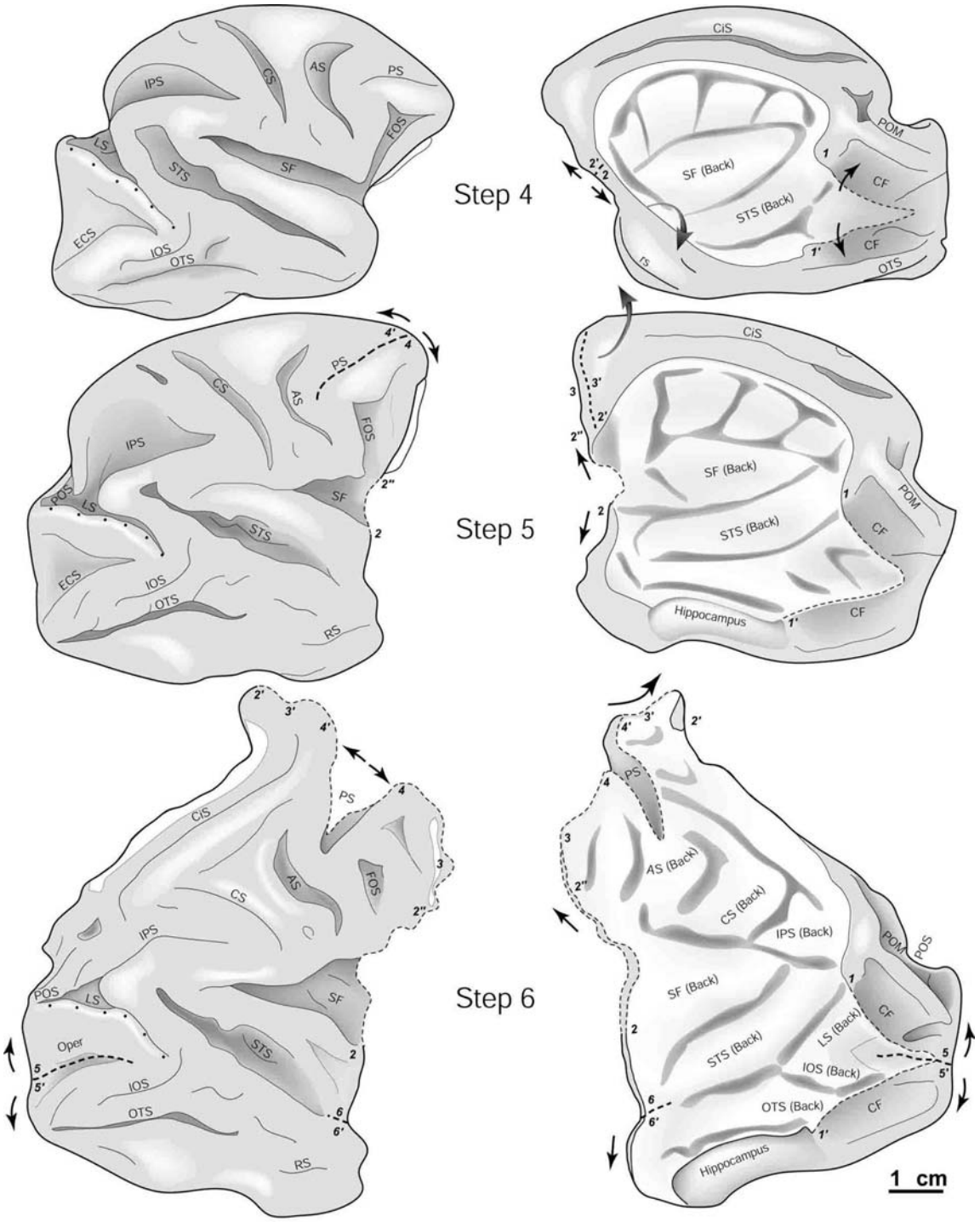

Fig. 1 continued. Part 2 continued. *Step 5, Lateral view:* The relieving cut is extended from (*4,4'*) along the fundus of the principal sulcus (PS) (dashed line) to flatten frontal cortex. This cut moves *2'* and *2''* (which started out adjacent) far apart. *Step 6:* The first relieving cut continues from (*5,5'*) to bisect the occipital operculum (horizontal meridian representation in V1). The lunate sulcus (LS) and posterior occipital sulcus (POS) are now easily accessible. The third and final relieving cut is made from (*6,6'*) to the end of the superior temporal sulcus (STS).

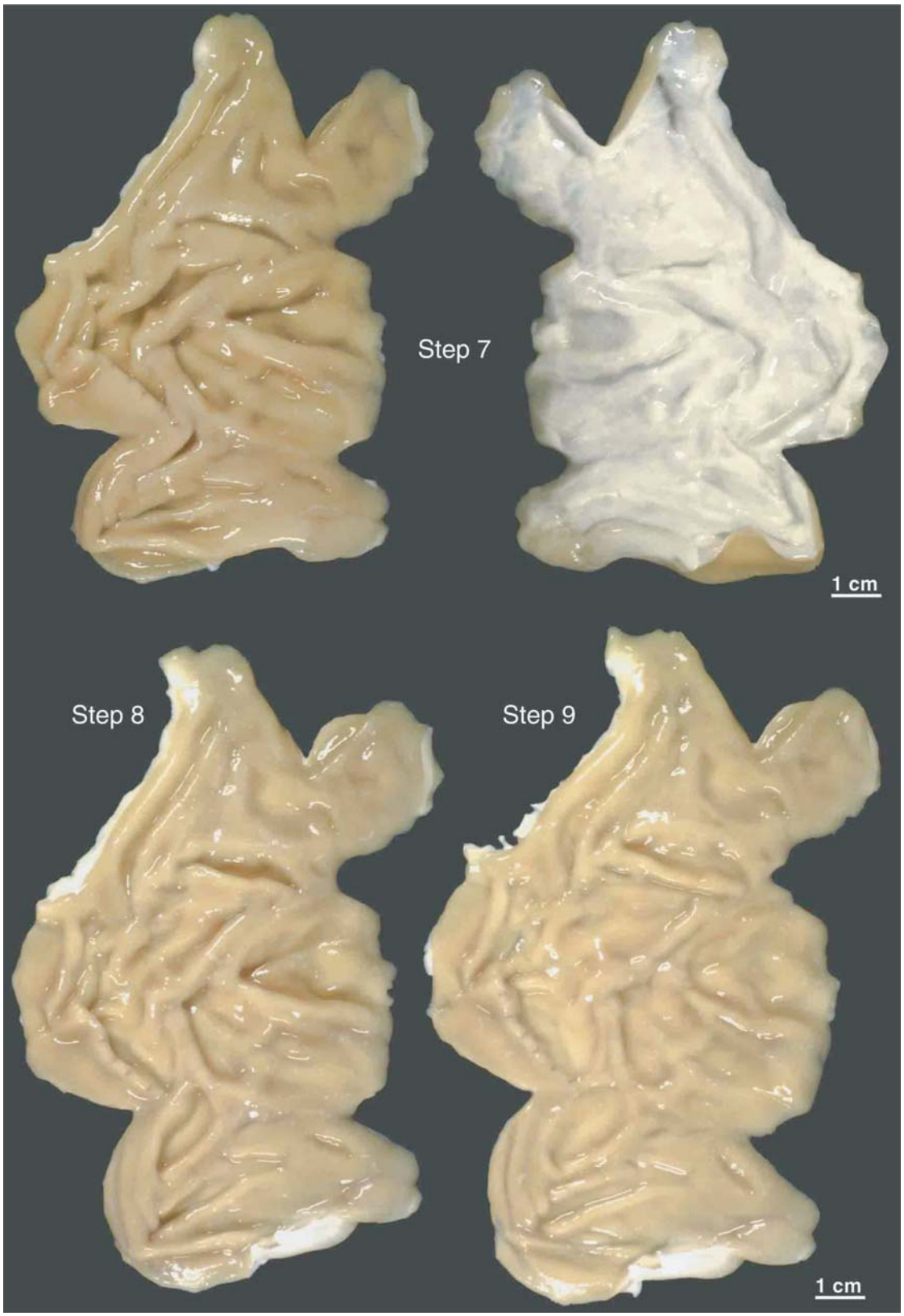

Fig. 1 continued. Part 3. *Step 7*: The cortex is further flattened by removal of white matter from the lunate and the inferior-occipito sulcal (IOS) regions. The bulb of the hippocampus is unfurled from the white matter (curved arrow). *Step 8*: Further relaxation is achieved by rubbing a moistened swab against the white matter to strip it from the cortical sheet. If the white matter is overfixed, a blunt microspatula can be used instead, at some risk of puncturing the flatmount.

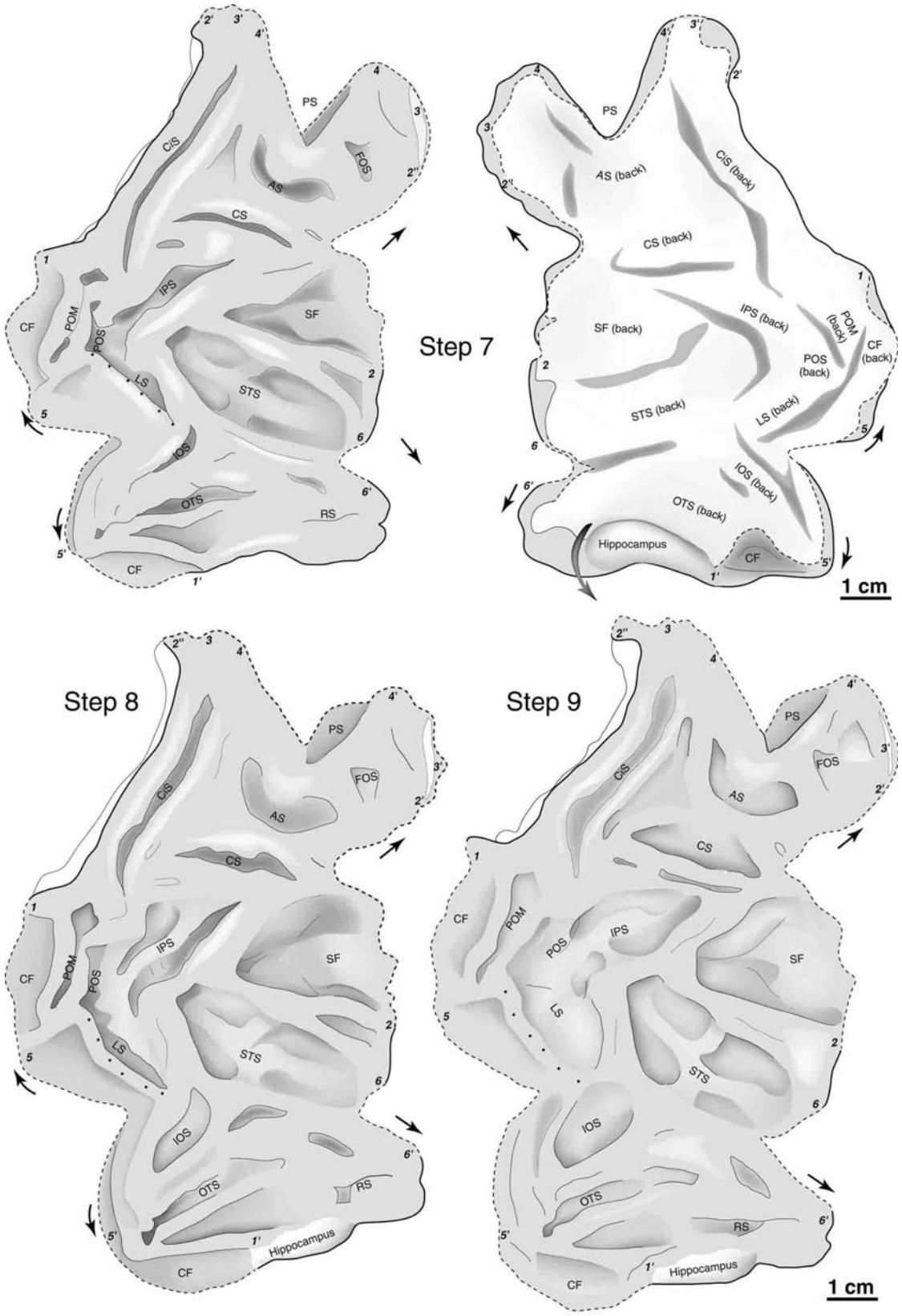

Fig. 1 continued. Part 3 continued. Residual pia-arachnoid is stripped away and the flatmount is gradually worked into a flatter configuration by gently pulling its edges outward on a 5 x 7 inch glass slide. *Step 9:* Completely unfolded cortical hemisphere, just prior to application of weight.

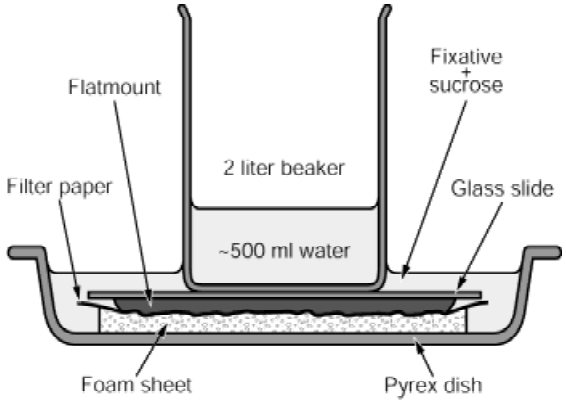

Fig. 2. To flatten the cortex, the pial surface is pressed against a glass slide, while the white matter surface sits on a soft, deformable sheet of foam, covered with a sheet of filter paper. The fixative and sucrose are able to diffuse through the foam, cryoprotecting and postfixing the specimen.

After the xylene had evaporated, the paper was peeled away, transferring the grid pattern onto the glass slide.

Each 2 × 2 mm square filled the field of view at 100× in a Zeiss microscope. Using a camera lucida attachment, we focussed on the bottom of the slide to align the edges of the counting square with a 200 × 200 mm square on a sheet of standard 8.5 × 11 inch paper. We then focussed on the plane of the tissue specimen (the grid created no interference) and viewed it through crossed polaroid filters to reveal CTB-filled cells. The location of every labeled cell was marked, and every box in the flatmount was surveyed. Individual sheets were taped together to yield a giant quilt that covered the laboratory floor, showing the location of each cell in a single section from the flatmount.

Results

Analysis of complete macaque flatmounts

Fig. 3 shows the flattened cerebral cortex just prior to cutting with a freezing microtome. The sulci and gyri have been eliminated by the transformation of the cortex into a flat sheet of tissue. The location of sulci could nonetheless be determined by referring to the photographs taken during each stage of the flatmounting process. We defined the boundary between sulci and gyri as the line where the tissue disappears from surface view in the intact brain. The position of minor grooves and cracks in the tissue surface also helped to locate sulcal borders, because they often occurred at the transition between sulci and gyri. In this example, the total flatmout surface area was 8867 mm^2 (8721 mm^2 cortex and 146 mm^2 hippocampus). The gyri accounted for 67% and the sulci represented 33% of the cortical surface area. The flatmount yielded a total of 17 sections, each 65 μm thick. The total thickness, only 1.1 mm, indicates that some compression of the cortex occurs during the application of weight to flatten the surface.

Fig. 4 shows the flatmounting process for the largest hemisphere we encountered among ten animals. It measured 14,353 mm^2 (14,113 mm^2 cortex and 240 mm^2 hippocampus). In Fig. 4, each gyrus is depicted on the surface of the intact hemisphere and on the flatmount. This helps to visualize the spatial transformation involved in rendering the cerebral hemisphere into a flat sheet of tissue. The gyri in this animal accounted for 54% of the cortical surface area.

In a third monkey, with an intermediate-sized flatmount (11,049 mm^2 cortex and 181 mm^2 hippocampus), the gyri occupied 59% of the cortex. These three examples reflect a trend: in animals with a greater cortical surface area, a greater proportion of the tissue was situated within sulci. Animals with a larger cortex appear to achieve tissue expansion mostly by enlargement of their sulci, rather than their gyri. This makes sense, because enlargement of gyri would require enlargement of the skull. In Fig. 5, all three flatmounts have been superimposed, to provide a sense of the variation in relative size and location of the sulci. A mean of 60% of the cortical sheet was occupied by gyri in the macaque.

The mean flatmount surface area was 10,611 mm^2 (S.D. 1897 mm^2) (Table 1). Areal shrinkage due to fixation was unknown, but was probably $< 5\%$, because the tissue was so lightly fixed (Mouritzen Dam, 1979). The mean cortical surface area was 10,430 mm^2 (S.D. 1859 mm^2). The remainder was hippocampus (mean area 181 mm^2). The mean cortical flatmount shape (Fig. 6) was determined by averaging the outlines of eight flatmounts, each prepared according to the sequence of relieving cuts described in Fig. 1. The shapes of V1 and V2, easily delineated by their distinctive CO staining patterns, were also averaged. In every specimen, strong CO staining was also visible in the MT (V5) complex (in the superior temporal suclus), auditory cortex (in the Sylvian fissure), and somatosensory cortex (in the central sulcus). These CO-rich areas were outlined by eye, and then averaged to indicate their relative size and location.

Total flatmount area ranged by a factor of 1.7, from 8395 mm^2 to 14,353 mm^2. V1 and V2 also showed considerable variability, ranging by a factor of almost 2 in surface area. On average, they accounted for 12.8% (V1) and 9.7% (V2) of the total cortical surface area. The relationship between V1, V2, and total cortical surface area is plotted in Fig. 7. The correlation between V1 area and total cortical area was 0.97 (Pearson product-moment correlation, $P < 0.001$). The correlation between V2 area and total cortical area was 0.93 ($P < 0.001$). The correlation between hippocampus area and total cortical area was 0.79 ($P < 0.01$). V1 area and V2 area were also well correlated ($r = 0.87$, $P < 0.002$). These data indicate that animals with a large cerebral cortex have a correspondingly large V1, V2, and hippocampus. Similar analyses for the CO-rich patterns in area MT, auditory cortex, and somatosensory cortex yielded only a weakly positive correlation with overall cortical area. This may be due to the fact that CO does not delineate sharply the borders of these regions, making detection of a correlation difficult. On the other hand, Maunsell and Van Essen (1987) have previously noted the lack of a close correlation between V1 and MT surface areas.

It is interesting to compare our mean flatmount, generated by actual physical flattening of the cortex, with a virtual flatmount prepared by computer reconstruction. Fig. 8 shows the most recent, published version of the macaque cerebral cortex flattened with the aid of a computer by Van Essen and colleagues (Drury et al., 1996; Lewis & Van Essen, 2000; Van Essen et al., 2001). The computer flatmount has a rounder overall shape. Area V2 accounts for 8.6% of the total cortex, close to the mean percentage occupied by V2 in our physical flatmounts. However, area V1 is much larger in the computer flatmount than the physical flatmount (15% *vs.* 12.8%).

The gyri represent a smaller percentage of the cortical surface area in the computer flatmount. They occupy 46% of the cortex (Fig. 8), compared with a mean of 60% in our flatmounts. Certain gyri appear unusually narrow in the computer flatmount. For

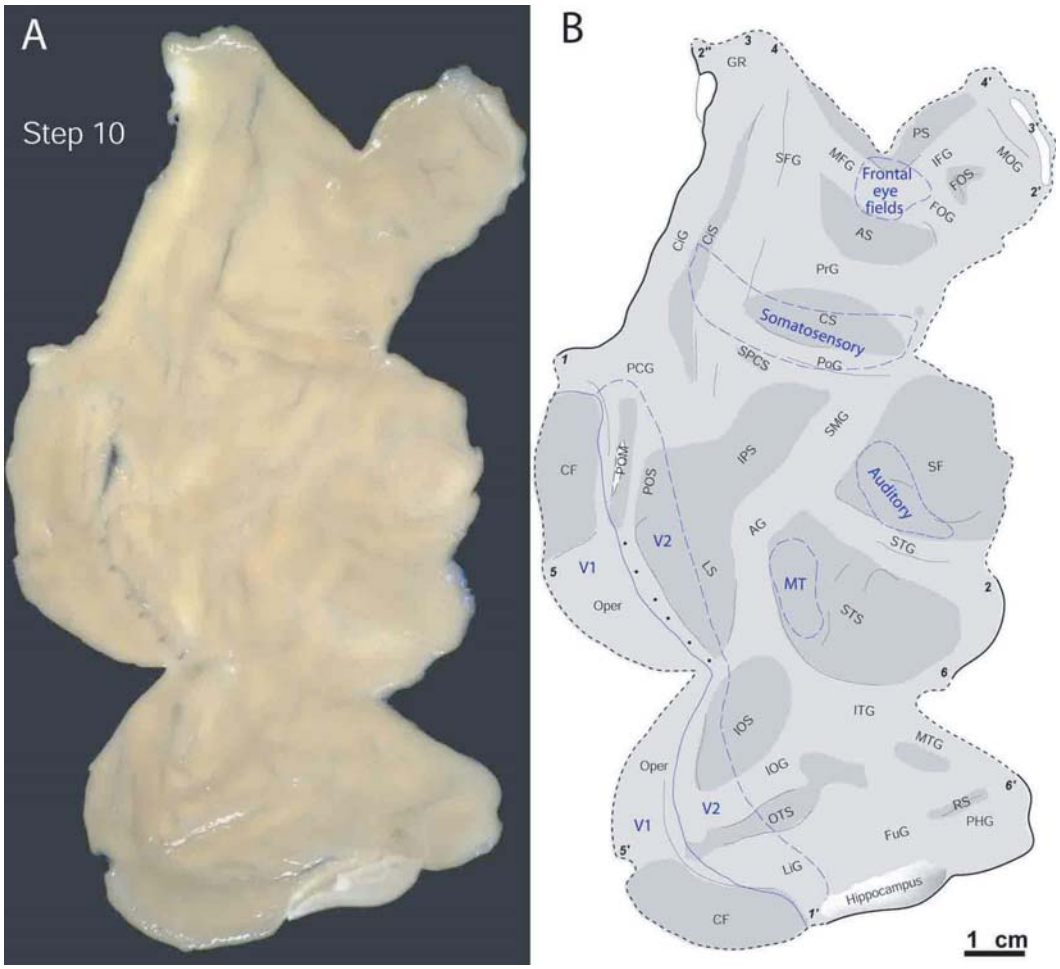

Fig. 3. A: Monkey 1. *Step 10:* Appearance of the cortical sheet, after flattening and post-fixation. B: Diagram showing the sulci (dark gray) and gyri (light gray), ascertained from photographs taken at each stage in the unfolding process. The solid lines denote the natural edge of the cortex; dashed lines mark relieving cuts. Note that adjacent points (e.g. *1,1'* and *2,2''*) become widely separated by flatmounting. Dots represent tracer injection sites in V2. Cortical areas (blue dashed lines) were delineated by their CO patterns (see Fig. 10).

example, the superior temporal gyrus and the angular gyrus are reduced to only ~ 2 mm wide. We have measured their minimum width in several intact brains and obtained about 5 mm.

The shape of a flatmount depends greatly on the placement of relieving cuts in the cerebral hemisphere. The computer flatmount (Fig. 8) was generated by making three relieving cuts, in addition to the V1 relieving cut. The location and extent of these three relieving cuts were not specified (Drury et al., 1996). In our standard flatmount, three relieving cuts are made, as illustrated in Fig. 1. Their placement gives our flatmount a more rectangular overall shape.

To illustrate further how flatmount shape can be influenced by relieving cuts, we illustrate two specimens prepared according to a different sequence of cuts. In the first flatmount we attempted, V1 was left intact by making relieving cuts parallel to the V1/V2 border (Fig. 9A). In this preparation, as in the original Felleman and Van Essen (1991) reconstruction, V1 hangs from the hemisphere by the foveal representation. It constituted 12.2% of the total cortical area (compared with a mean of 12.9%), suggesting that less stretching of V1 occurs when relieving cuts are made around the outside of V1. The alternative approach, splitting V1 along the horizontal meridian, results in some enlargement of V1 because it must be stretched to maintain apposition to V2. This is also evident in computer flatmounts. For example, V1 occupies 13.2% of the whole cortex when prepared by making relieving cuts along the V1/V2 border (see Case 79-0, Fig. 9A, Drury et al., 1996). When the very same case is flattened, instead, by making a relieving cut down the middle of V1 (Fig. 8), the area of V1 increases to 15.0% of the cortex (a 14% enlargement).

In Fig. 9B, the tissue tore along the medial edge of the V1 operculum while the relieving cut was being made along the fundus of the calcarine fissure. An isolated piece of dorsal calcarine V1 remained attached to the cingulate cortex, ending up far from the rest of V1. A deep tear also occurred inadvertently in cingulate cortex. As a result, the flatmount had a rather anomalous shape, but nonetheless it yielded vivid CO staining patterns.

For many experiments, it may be unnecessary to flatten the entire cerebral cortex. It is easier to handle smaller sections,

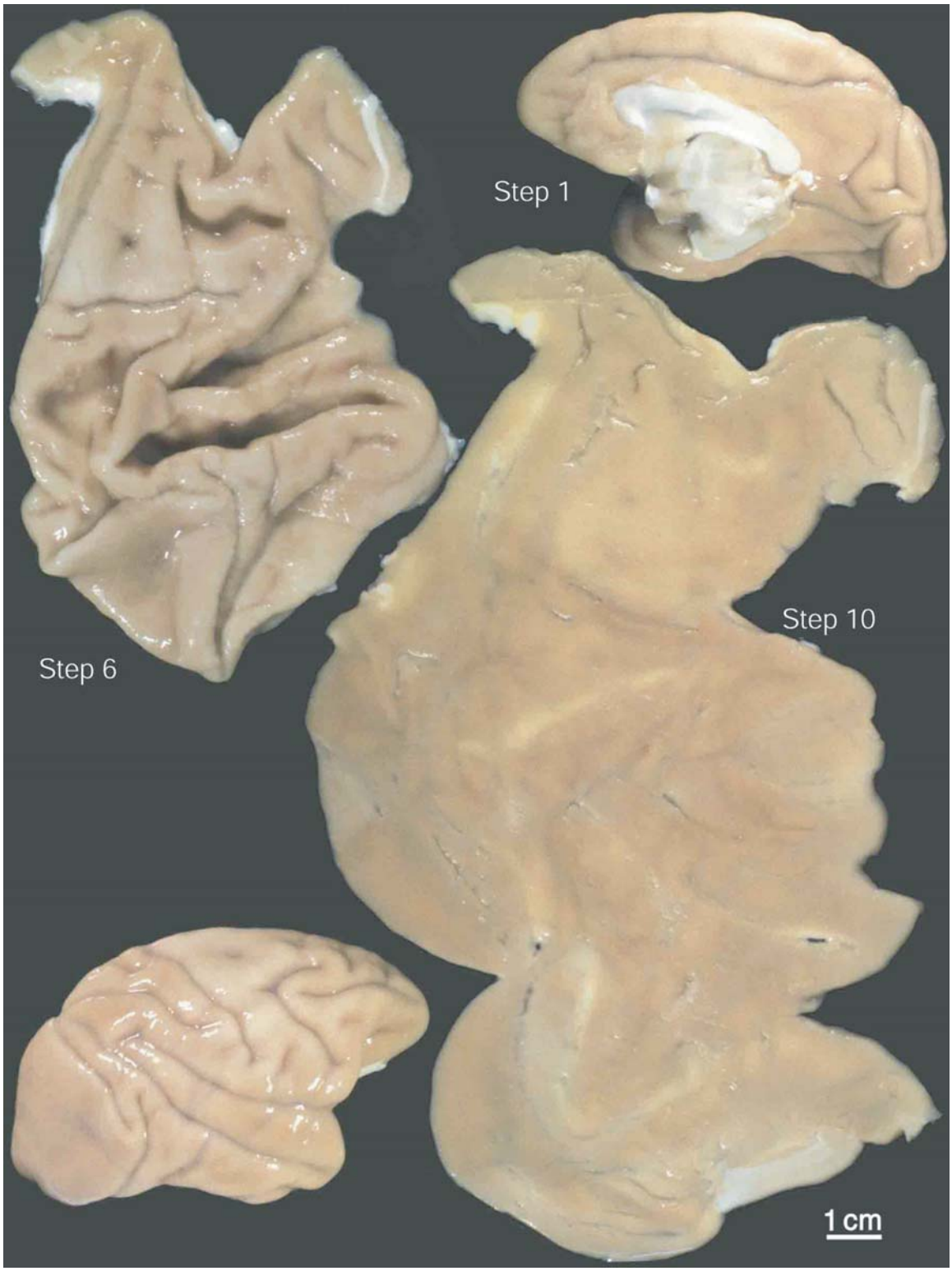

Fig. 4. Monkey 2. Flatmount of the largest specimen in our series (14,353 mm^2), a Rhesus macaque, with the gyri indicated with color coding, both on the intact hemisphere and the flatmount. Grey regions denote sulci, which accounted for 46% of the cortical surface in this hemisphere. Comparison with the flatmount with Fig. 3A underscores the variation in cortex surface area from animal to animal.

especially if they must be processed floating in solutions, rather than slide-mounted. Fig. 9C shows a partial flatmount, containing just the calcarine fissure, operculum, lunate sulcus, angular gyrus, superior temporal sulcus, and inferior occipital sulcus. The relieving cut along the V1 horizontal meridian has been eliminated. In this animal, the cortices were removed without bisecting the cerebral hemispheres, leaving intact the brainstem, cerebellum, thalami, and basal ganglia for sectioning in a single block.

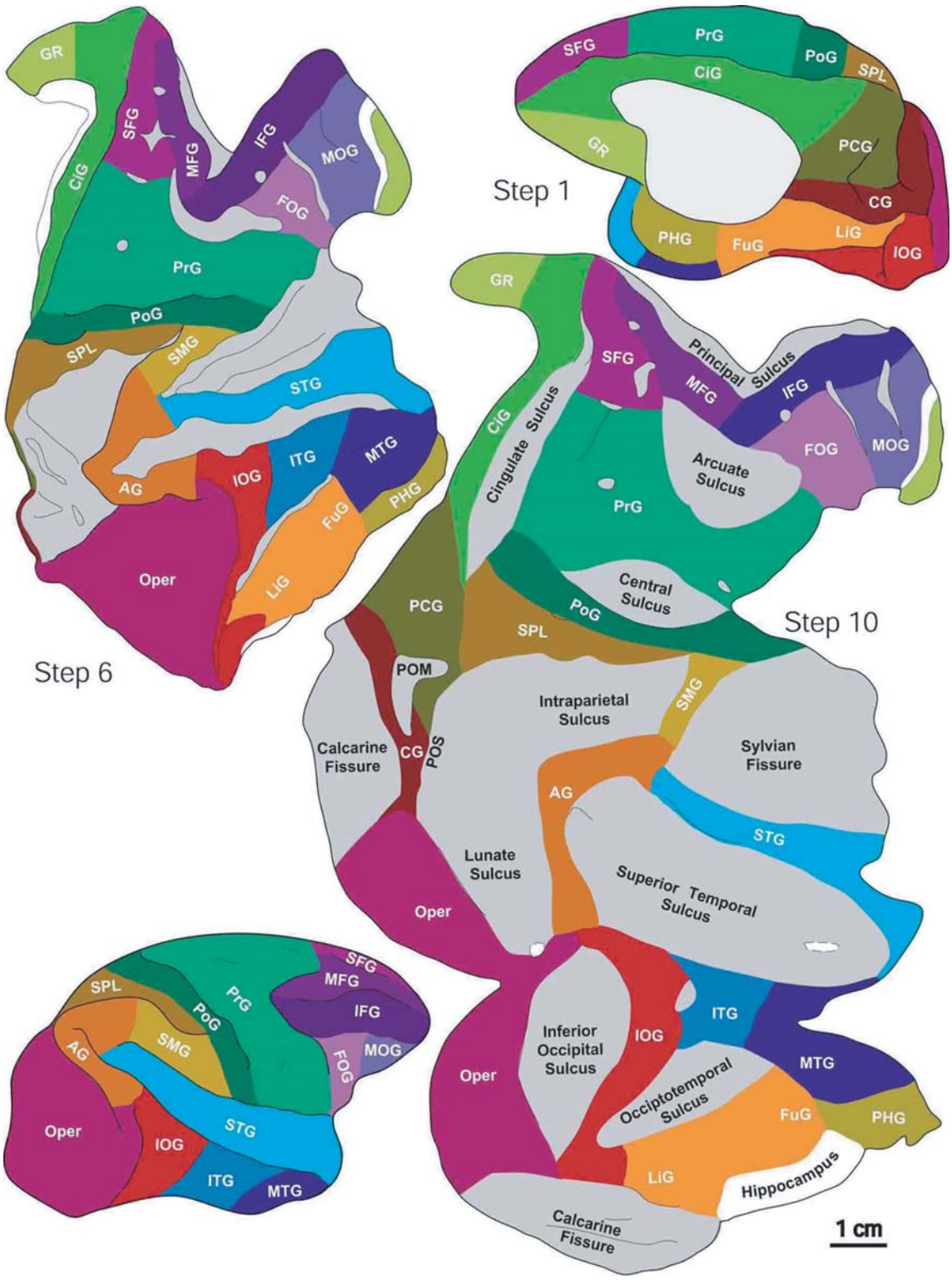

Fig. 4 continued.

Cytochrome-oxidase patterns in cortical flatmounts

V1 and V2 have distinct borders in CO-stained flatmounts, making it possible to define their areas precisely (Fig. 10). In each specimen, V2 was divided into dorsal and ventral halves by drawing a line across it at the foveal representation, where it is thinnest. In our sample of ten flatmounts, there was no overall difference in the surface area of dorsal and ventral V2 (505 mm^2 *vs.* 507 mm^2). However, distortion from the flatmounting process made ventral V2 appear wider and more curved.

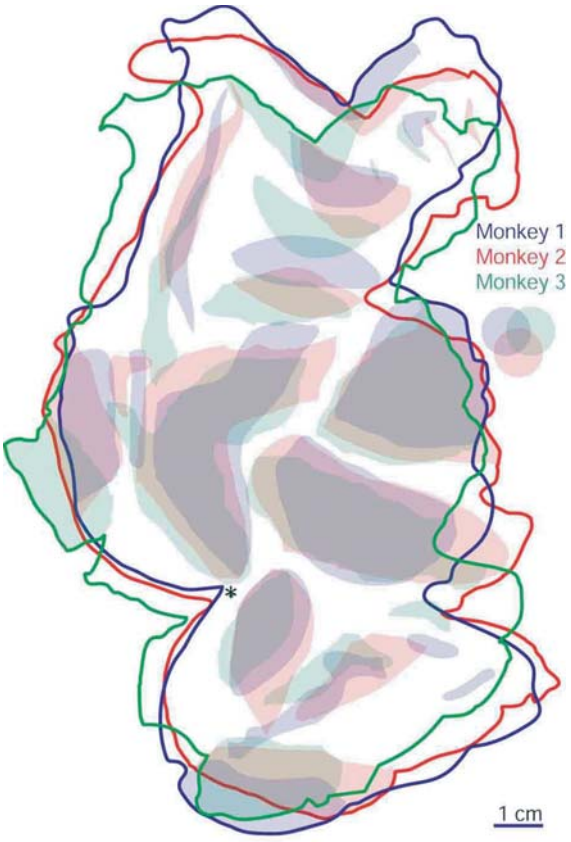

Fig. 5. Flatmount outlines of the right hemisphere from three animals, superimposed to show variability in overall shape, and in the location of sulci (shaded regions). The flatmounts were normalized to the mean surface area (10,611 mm^2) by expanding Monkey 1 (120%), and by contracting Monkey 2 (74%) and Monkey 3 (94%). They were then superimposed at the representation of the fovea in V1/V2 (asterisk). This point was located in CO sections by finding the point along the V1/V2 border at the apogee of V1 where V2 was thinnest. The flatmounts were then rotated to achieve maximum overlap. Increasing scatter in the location of the central, arcuate, and principal sulci is due simply to alignment of the sections on a more distant point (the fovea in V1/V2).

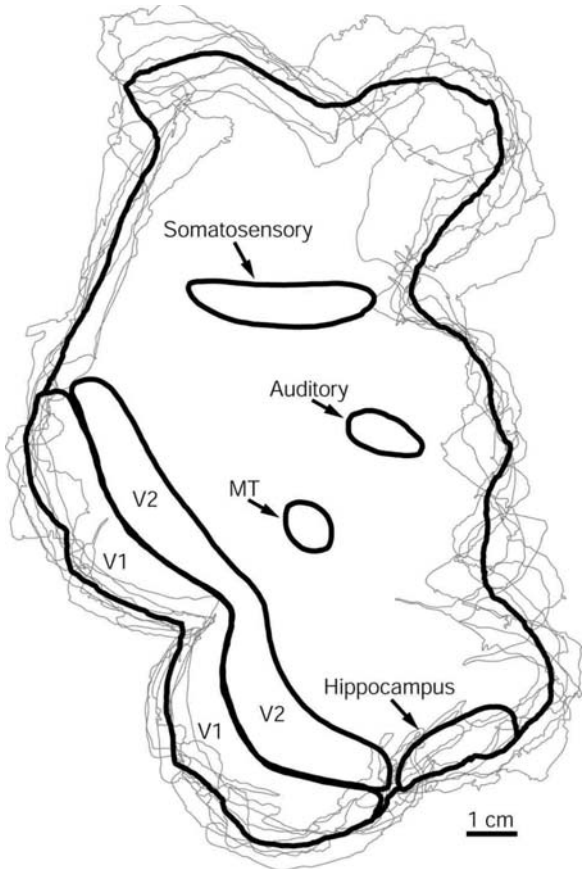

Fig. 6. Mean shapes (black outlines) of the complete flatmount, V1, V2, hippocampus, MT complex, auditory cortex, and somatosensory cortex in the right hemisphere of the macaque, superimposed on eight individual specimens (thin lines). The figure was compiled by reflecting the two left flatmounts, normalizing each flatmount to the mean area of 10,611 mm^2, aligning the specimens at the V1/V2 foveal representation, rotating the specimens to maximize overlap, and blending them sequentially in pairs (Blend Tool, Adobe Illustrator 9.0). The final result, a "mean flatmount", lacks the sharp angles created by relieving cuts, but gives a fairly accurate impression of the general shape of the cortical flatmount, as well as the size and position of various areas.

The intrinsic CO staining pattern of V1 requires no mention, because it has been fully described previously (Horton & Hubel, 1981; Horton, 1984; Wong-Riley & Carroll, 1984). V2 contains coarse parallel CO stripes (Horton, 1984), organized into a repeating pattern of pale-thin-pale-thick (Tootell et al., 1983). Fig. 11 shows the complete pattern of CO stripes in two flatmounts. In one example, there were about 34 cycles of stripes in V2 (17 dorsal V2, 17 ventral V2). The exact number of cycles was a matter of interpretation, because they occasionally bifurcate or break into fragments. The V1/V2 border measured 140.0 mm, yielding 4.1 mm per cycle. Thin stripes in the representation of the peripheral visual field had a slimmer, more irregular appearance than those in the central visual field. We have also observed this eccentricity-dependent change in the appearance of the thin stripes in squirrel monkeys (Fig. 12), so it does not appear to be a peculiarity limited to the macaque. In the squirrel monkey, we have flattened V1 in a single piece, so the differing appearance of peripheral versus central V2 thin stripes cannot be attributed to splitting V1 down the middle.

Although CO stripes are present in every macaque, their clarity varies inexplicably from animal to animal. In many specimens, dark stripes cannot be differentiated clearly into thick versus thin. The complete pattern of V2 stripes could be reconstructed with confidence in only two other macaques. Their flatmounts contained 26 and 28 cycles of V2 stripes, measuring 4.2 and 4.8 mm/cycle, respectively. In these specimens, the thin stripes also displayed a more dotted appearance in the peripheral field representation.

We searched carefully for a CO pattern that might identify the next visual area, anterior to dorsal V2, which has been dubbed area "V3" or "DM" (Zeki, 1978; Beck & Kaas, 1999; Lyon & Kaas, 2002). Fig. 13 shows a wedge-shaped region, about 22 mm long by 6 mm wide, with a surface area of 103 mm^2, containing a distinctive CO pattern. It consisted of about seven pairs of dark and pale stripes, each 1-2 mm wide, oriented perpendicular to the border with V2. These stripes were wider than those in V2. A fine, speckled pattern of CO activity was also present, scattered through both pale and dark stripes. No such distinctive pattern of CO activity was visible anterior to ventral V2.

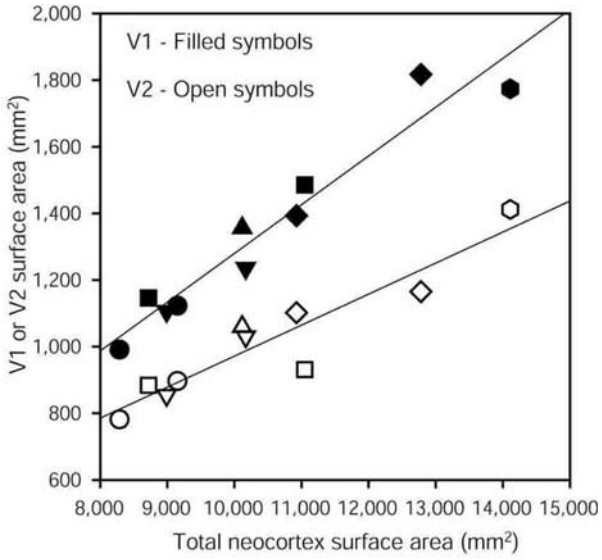

Fig. 7. Graph of total cortical surface area versus V1 or V2 surface area for ten hemispheres. Different symbols indicate individual monkeys. V1, V2, and total cortical area are strongly correlated.

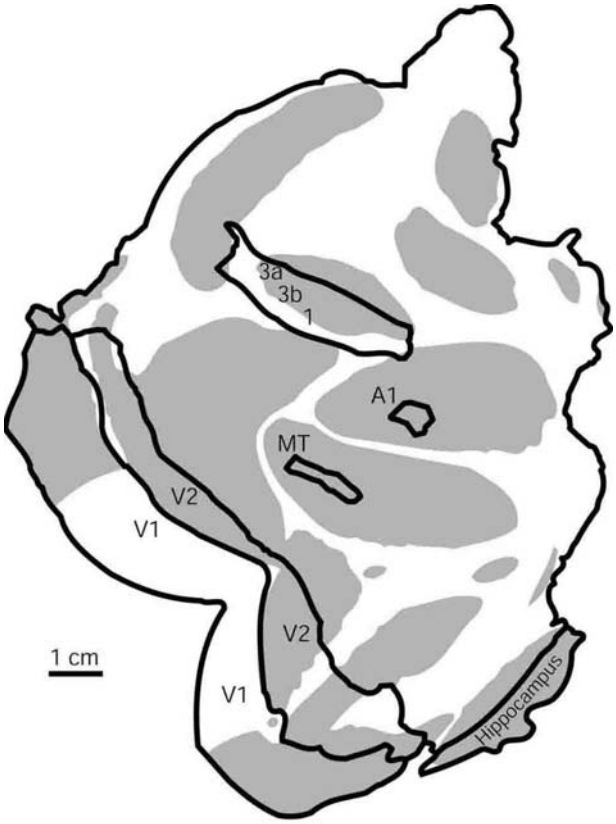

Fig. 8. Computer-based flatmount, adapted from Van Essen (Lewis & Van Essen, 2000, Fig. 12G; Van Essen et al., 2001, Fig. 1E), scaled in size to the mean physical flatmount in Fig. 6 by enlarging it 116% from 7923 mm^2 to 10,611 mm^2. Sulci are marked by gray shading. Areas MT, A1, and 1, 3b, 3a are shown as delineated by Van Essen and coworkers. The CO-rich patterns we have identified in physical flatmounts probably include these areas, but may not correspond exactly. Comparison with the physical flatmount in Fig. 6 reveals striking similarities and differences. See Van Essen (2003) for another version of the macaque map.

This distinctive CO staining pattern may correspond to "V3/DM", but it was seen with such clarity in only a single animal. In the other eight animals, we saw only a murky pattern of crude dark/pale stripes with vague borders, akin to that described by others (Tootell & Taylor, 1995; Lyon & Kaas, 2001). It could not be used reliably to establish the boundaries of "V3/DM". This was a disappointment, because our effort to identify a pattern of CO staining that would reveal area "V3/DM" consistently was a primary motive for embarking on this flatmount study.

A pattern of dark CO staining associated with area MT has been identified previously (Horton, 1984; Tootell et al., 1985; Krubitzer & Kaas, 1990; Tootell & Taylor, 1995). It has indistinct borders, making it uncertain if the CO pattern corresponds strictly to area MT, or includes nearby, putative visual areas (e.g. "MST," "FST," "V4t"). The dark CO staining in MT demonstrated marked inter-animal variation. In some animals, the pattern consisted of dots measuring about 250 μm in diameter, spaced about 1 mm apart, organized into an irregular grid (Fig. 14A). In other animals, the CO pattern formed crude parallel bands (Fig. 14B). With the Gallyas stain (Fig. 14C), adjacent sections exhibited strong myelin content, typical of area MT. The dark myelin bands matched the pale CO bands, as previously demonstrated in area V2 (Horton & Hocking, 1997). The CO pattern in area MT was visible in all layers, but seen best in the middle and superficial layers. Its functional significance remains unknown.

A zone of prominent CO activity was visible in the Sylvian fissure in every flatmount (Figs. 10 & 15). It consisted of 4-5 parallel bands of dark CO activity, about 10 mm long and 0.5 mm wide, each separated by a pale gap of comparable size. It corresponds to the primary auditory cortex (A1), but may also include portions of surrounding auditory fields (Tootell et al., 1985; Jones et al., 1995; Clarke & Rivier, 1998).

The final area containing conspicuously robust CO activity was primary somatosensory cortex (S1) (Fig. 10). It consisted of a CO-dense region, about 50 mm wide by 8 mm across, straddling the postcentral gyrus and the central sulcus (Fig. 16). It was recognized first in flatmounts of owl monkey cortex (Tootell et al., 1985). Cross sections of macaque and human somatosensory cortex show strong CO activity in areas 3a, 3b, and 1 (Eskenasy & Clarke, 2000; Jones et al., 2002). The dark region of CO activity present in macaque flatmounts corresponds to these areas, and may also include area 2.

V2 connections mapped in cortical flatmounts

CTB was injected in dorsal V2 in three hemispheres to label all cortical regions that project to area V2. A string of six injections, each about 1 mm in diameter after silver intensification, was made at a depth of 600 μm along the lower vertical meridian representation. Tracer was present at the injections sites from layer 1 to 6, but did not extend into the white matter.

Fig. 17 shows the distribution of labeled cells in a single section. This section is from the hemisphere used to illustrate the flatmounting process (Fig. 1). There were 35,721 cells filled retrogradely. V2 had 28,064 labeled cells, reflecting the fact that most tracer was transported locally. V1 contained 4905 cells and MT 183 cells. The remaining 2569 labeled cells were located in other areas (e.g. "V3", "V4", etc.). The relative amounts of labeled cells in various cortical areas is dependent on layer, and hence, on the depth of any given section. More superficial sections passing through the CO patches in layers 2/3, for example, contained

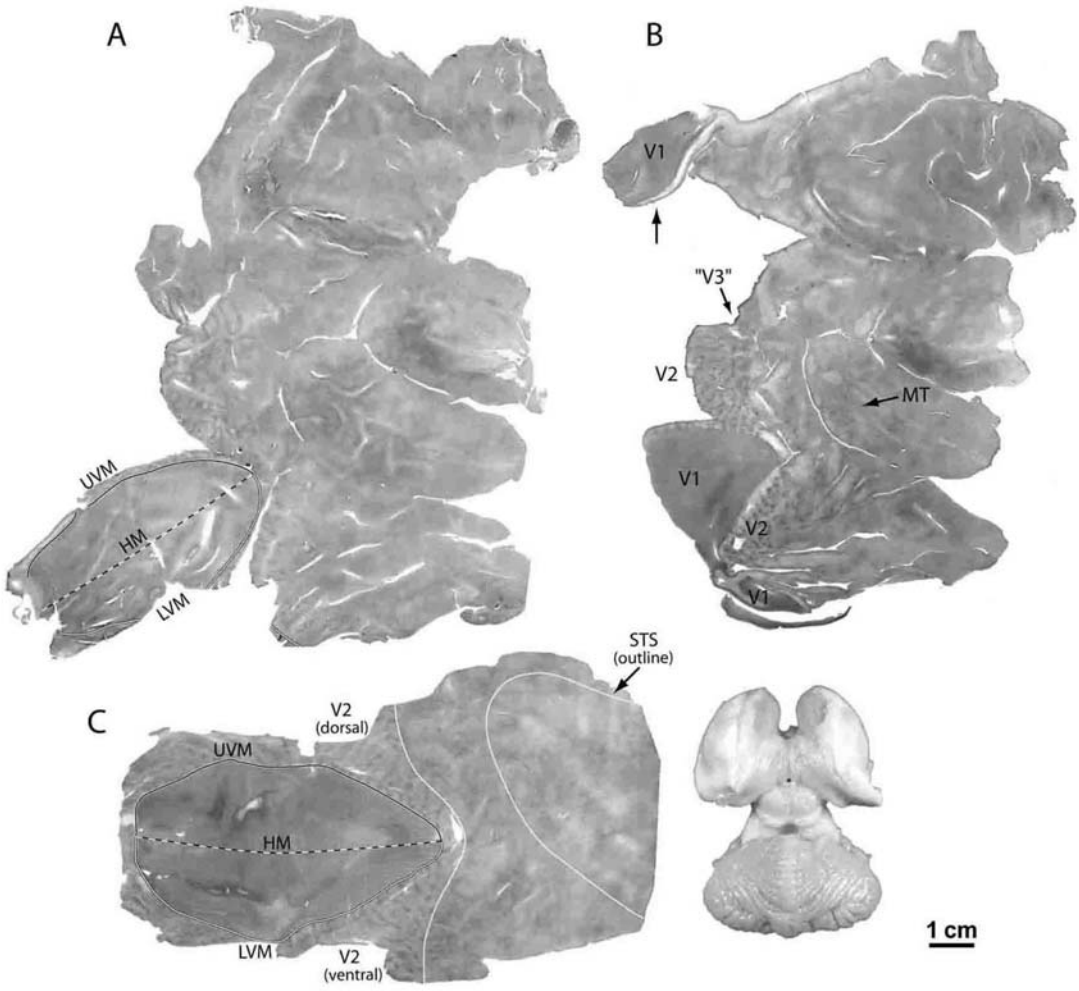

Fig. 9. A: Monkey 4. CO-stained section from a flatmount prepared by making a relieving cut parallel to the V1/V2 border, leaving V1 in a single piece. The V1/V2 border contains the representation of the vertical meridian (LVM = lower vertical meridian, UVM = upper vertical meridian); V1 is bisected by the horizontal meridian (HM). B: Monkey 5. CO-stained section from a flatmount where V1 tore along the medial edge of the operculum, leaving a large piece of calcarine V1 (arrow) attached to cingulate cortex. "V3" and MT regions are shown at higher power in Figs. 13 and 14, respectively. Neither of these two flatmounts was used to prepare the mean flatmount in Fig. 6, because their relieving cuts were placed differently. C: Monkey 10: Partial flatmount, stained for CO, used to map connections between V1, V2, MT, and subcortical structures (right). By preparing only a partial flatmount, we avoided bisecting V1. In this animal, a Rhesus macaque, V1 was enormous (1950 mm^2); it is not incorporated in Table 1 or Fig. 7 because a complete flatmount was not prepared. It is worth noting that the three specimens with the largest V1 surface area were Rhesus, suggesting that cortical surface area may be greater in *M. mulatta* than *M. fascicularis*.

greater numbers of labeled cells in V1. Nonetheless, these numbers give some impression of the relative strength of inputs to V2. The feedforward projection from V1 was about twice as strong as the entire feedback projection from higher visual areas.

By placing six injections along the representation of the lower vertical meridian, from 0 deg to 10 deg, we hoped to identify six discrete loci of retrogradely filled cells along the vertical meridian in each cortical area projecting to V2. Such a strategy would aid in mapping the boundaries of extrastriate visual areas. In fact, only V1 contained six tidy clusters of labeled cells. In other cortical regions the distribution of labeled cells was usually patchy, but there were never six clusters corresponding to the six tracer injections. The reason, presumably, is that feedback projections are divergent. For example, the six tracer injections filled < 1% of V2, but resulted in clumps of labeled cells throughout 10% of area MT (judged by reference to its dark CO staining pattern). This discrepancy implies that single MT neurons project over a wide area in V2, thereby obscuring any tendency for six injections in V2 to produce six foci of labeled cells in MT.

Another factor is that compartments within any given cortical area often differ in their projections to other cortical areas. Only the thick stripes of V2 are thought to be interconnected with MT (DeYoe & Van Essen, 1985). In the example shown in Fig. 17, only one of six injections landed in a thick V2 stripe. Therefore, only a single field of retrogradely filled cells should have been expected in MT. However, we found four discrete clusters of cells. This probably reflects an intrinsic columnar arrangement of V2-projecting cells within MT. All these factors conspire to make it difficult to use cell projection patterns to recognize the boundaries of extrastriate visual areas.

Using a sensitive tracer like CTB in giant flatmount sections creates a practical problem, namely, how to document the distri-

Fig. 10. Monkey 1. CO-stained section, #6, from the flatmount illustrated in Fig. 3A, after silver intensification, showing six CTB injections near the lower vertical meridian in V2. Areal boundaries are sharply defined by CO only for areas V1 and V2. Dark CO patterns are present in other areas, such as MT, somatosensory, auditory cortex, the frontal eye fields, but cannot be used to define exact boundaries.

bution of literally hundreds of thousands of retrogradely filled cells in each hemisphere. Plotting the exact location of each cell is not practical, because it takes weeks for each section. As an alternative, one can scan systematically each section, using the grid to keep track of one's place, and note regions containing labeled cells. Fig. 18 shows where labeled cells were found in a survey of 11 sections, from layers 2-6.

In the lunate sulcus and angular gyrus, abundant cells were found in regions known by others as "V3, V3A, V4" or "DM, DI, DL" (Van Essen & Zeki, 1978; Beck & Kaas, 1999). In the intraparietal sulcus, a small projection was found in an area that could be either "LIP" or "VIP" (Felleman & Van Essen, 1991). In the superior temporal sulcus, many labeled cells were found in area MT. In addition, three other discrete fields of cells were present, one in the anterior bank (possibly "MST") and two inferolaterally along the sulcus floor and posterior bank (perhaps "FST"). A single, well-labeled zone of cells was present on the inferior occipital gyrus in an area known either as "TEO" (Desimone & Ungerleider, 1986) or "PITv" (Felleman & Van Essen, 1991). Finally, three distinct fields of cells were present in the fusiform gyrus and middle temporal gyrus. All the fields of labeled cells described in this hemisphere were observed in this animal's other hemisphere, and also verified in a single hemisphere from another animal.

Discussion

The deep convolutions of the brain surface in macaques and humans have impeded efforts to generate maps of the areas and connections of the cerebral cortex. In certain New World primates, such as the owl monkey, the cortex is less folded and many visual areas, such as V2 and MT, lie exposed on the surface rather than buried within sulci. For this reason, Allman and Kaas (1971, 1974, 1975) chose the owl monkey for their pioneering studies of the organization of extrastriate cortical areas.

A major advance in the effort to overcome the topological challenge presented by the brain's folds came with the development of methods for creating artificial surface views of the cortex from serial cross sections. This general approach involves transferring the outline of layer 4 onto a flat surface by systematically unfolding the contour of successive sections. It was first used by Hubel and Wiesel (1969) to reconstruct the two-dimensional pattern formed by ocular dominance columns in the calcarine fissure of the macaque. It was later refined by Van Essen and others to prepare maps of macaque extrastriate visual cortex (Van Essen & Zeki, 1978; Gattass & Gross, 1981), and eventually, the entire neocortex (Van Essen & Maunsell, 1980; Felleman & Van Essen, 1991). Originally, the contours of individual cross sections were aligned manually. Subsequently, computer-based approaches were employed to unfold and reconstruct the cortical surface (LeVay et al., 1985; Sherk, 1992). The preparation of computer-generated, two-dimensional representations of the convoluted cortical surface has been extremely useful for mapping areas in the macaque brain (Drury et al., 1996), for localizing fMRI activity in the human brain (Sereno et al., 1995; Dale et al., 1999; Fischl et al., 1999), and for interspecies comparisons (Van Essen et al., 2001; Brewer et al., 2002).

In the present study we have taken an alternative approach, namely, to produce a real, physical (as opposed to virtual, computer-reconstructed) flatmount of the entire macaque cerebral cortex. The cortex has been dissected from the white matter, unfolded, and flattened by making relieving cuts. The relieving cuts have been placed strategically, to achieve greatest flattening while preserving a maximally intact, optimally contiguous specimen. We have recorded photographically (Fig. 1) each step of the flattening process, providing a surface atlas of the gyri and sulci, so that one can see exactly how the intact cortex is rendered into a flatmount. If other laboratories decide to adopt the flatmount approach and make relieving cuts in the same places, it will facilitate comparison of data because all specimens will have the same, canonical shape. Preparation of complete flatmounts should be useful to anatomists who are mapping the cortical surface, and to physiologists who are curious about the internal anatomy of the sulci where they are placing their recording electrodes.

Flattening many macaque hemispheres using an identical approach has revealed a nearly two-fold range in the surface area of the neocortex. This remarkable range can be appreciated at a glance by comparing the flatmounts in Figs. 3A and 4 (step 10). There is also a two-fold variation in the surface area of individual cortical regions, for example, V1, V2, MT, S1, and A1 (Table 1), as shown previously (Brodmann, 1918; Penfield & Boldrey, 1937; Stensaas et al., 1974; Van Essen et al., 1981, 1984; Andrews et al.,

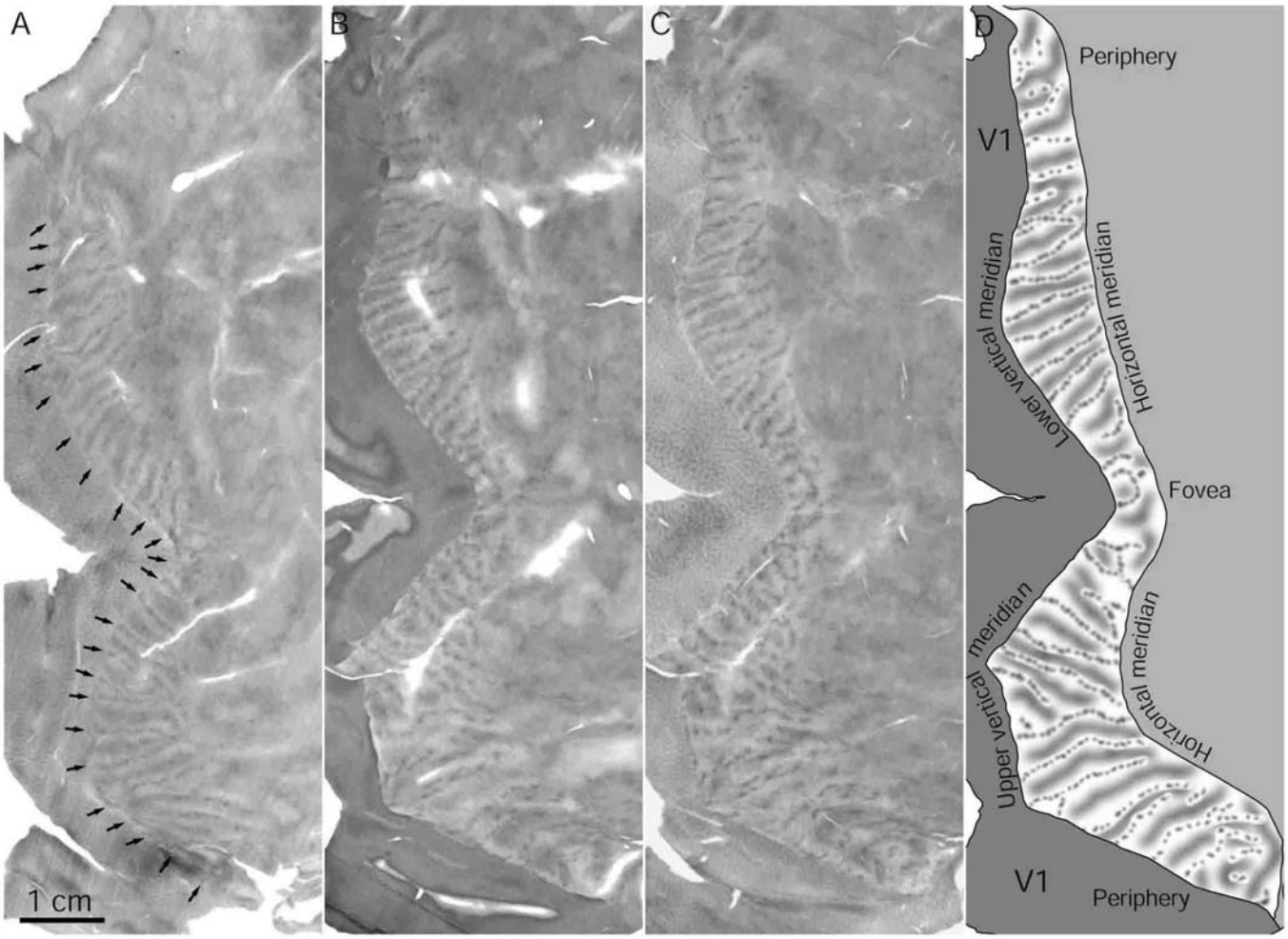

Fig. 11. A: Monkey 3. CO section showing the distinctive pattern of pale-thin-pale-thick stripes in V2. The thin stripes (arrows) are slightly darker than the thick stripes. Twenty-six cycles of stripes are present in this specimen. B: Monkey 6. CO section, from the only female in our series, showing another example of stripes in V2. C: Montage of the V2 stripes in B, compiled by including portions of adjacent sections to render a more complete view. Note that thin stripes in the periphery of V2 are more punctate and fragmented. D: Drawing of C showing ~ 34 cycles of stripes.

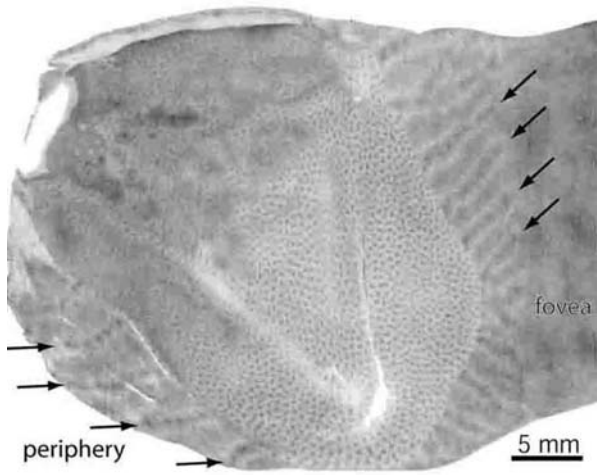

Fig. 12. Flatmount of a normal squirrel monkey, for comparison with the macaque, showing CO staining of the V2 stripes. Note the subtle difference in the appearance of the thin stripes (arrows) in the periphery versus fovea, a feature also present in the macaque.

1997). We now show that a correlation exists between the surface area of the entire neocortex and the surface area of individual regions (e.g. V1, V2). The biological significance of variation in cortical surface area is unclear. It may simply represent natural variation from subject to subject, with no functional correlate. Within a single species, no evidence exists to support the idea that animals with a larger V1 and V2 have better vision.

A major advantage of the flatmount technique for cortical mapping is that one can easily recognize "signature" patterns, such as the CO patches in V1, that are obscured when the brain is cut in cross section. In this report we have described characteristic CO patterns in macaque MT, A1, and S1. We have also shown the complete layout of CO stripes in single flatmount sections of V2. Previously, Olavarria and Van Essen (1997) flattened V2 in several pieces and found ~ 28 sets of stripes in their three most complete reconstructions. We have found a range from 26 to 34 sets, reflecting intrinsic variability in the number of cycles, analogous to the variability in the number of ocular dominance columns in V1 (Horton & Hocking, 1996). In the peripheral field representation of V2, we report that thin stripes are more irregular and dotted. If thin stripes are specialized for handling color information (Livingstone & Hubel, 1984; Roe & Ts'o, 1999), this change may

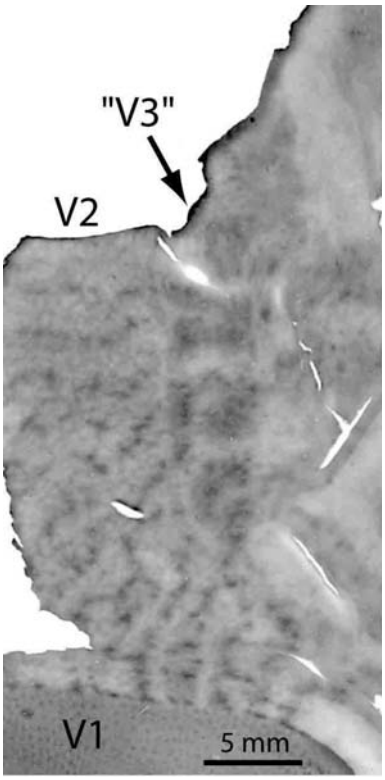

Fig. 13. Monkey 5. A distinctive pattern of CO activity from Fig. 9B, consisting of alternating light and dark stripes, that may correspond to area "V3". Note the pattern of CO staining in V2. Although robust, it cannot be differentiated easily into thick and thin stripes in this particular animal.

reflect reduced emphasis on color processing in the peripheral visual field.

In some animals the distinction between thick and thin stripes was difficult, or impossible, to discern. We believe that this is a genuine feature of the CO stripes in some macaques, and not an artifact of variation in the quality of histological processing. In primate cerebral cortex, the expression of columnar architecture is sometimes capricious. In squirrel monkeys, for example, clear cycles of pale-thin-pale-thick V2 stripes are present in every animal, but the occurrence of V1 ocular dominance columns is sporadic (Adams & Horton, 2003). Conversely, well-formed ocular dominance columns are present in every macaque, but V2 stripes are often poorly differentiated. It would be interesting to learn if projections from V1 to V2 are organized differently in macaques with weakly developed V2 stripes (Sincich & Horton, 2002*a*).

By preparing a flatmount of the entire hemisphere, one can readily trace the complete pattern of projections made by any area to all other areas within the cerebral cortex. To demonstrate the power of this approach, we injected a retrograde tracer, CTB, into area V2. Stepniewska and Kaas (1996) previously flatmounted a generous portion of macaque cortex and found projections to V2 originating in areas "DM", "DI", "DL" (also known collectively and roughly as "V3", "V3A", "V4"), V1, MT, "MST," "FST," "LIP," and "TEO." We have confirmed each of these projections, and in addition, report three projections to V2 arising from separate sites in the fusiform and middle temporal gyri (Fig. 18). These regions were not contained in the partial flatmounts prepared by Stepniewska and Kaas. Labeled neurons have been reported in the occipitotemporal sulcus and inferior temporal cortex after V2 tracer injection (Kennedy & Bullier, 1985; Rockland & Van Hoesen, 1994). Their location was not illustrated in these previous studies so one cannot determine if it corresponds to the sites we have identified. It is worth noting that every region sending a projection to V2 has been shown also to receive a projection from V2 (Gattass et al., 1997), except "FST" and the three fields in inferotemporal cortex.

One disadvantage of flatmounts is that determination of cortical layer is often more difficult than in cross sections. This problem is less serious in certain areas, where various staining methods produce characteristic laminar patterns. For example, CO has a typical laminar pattern of staining in V1 (Horton, 1984), and even in V2 (Sincich & Horton, 2002*b*), making it possible to

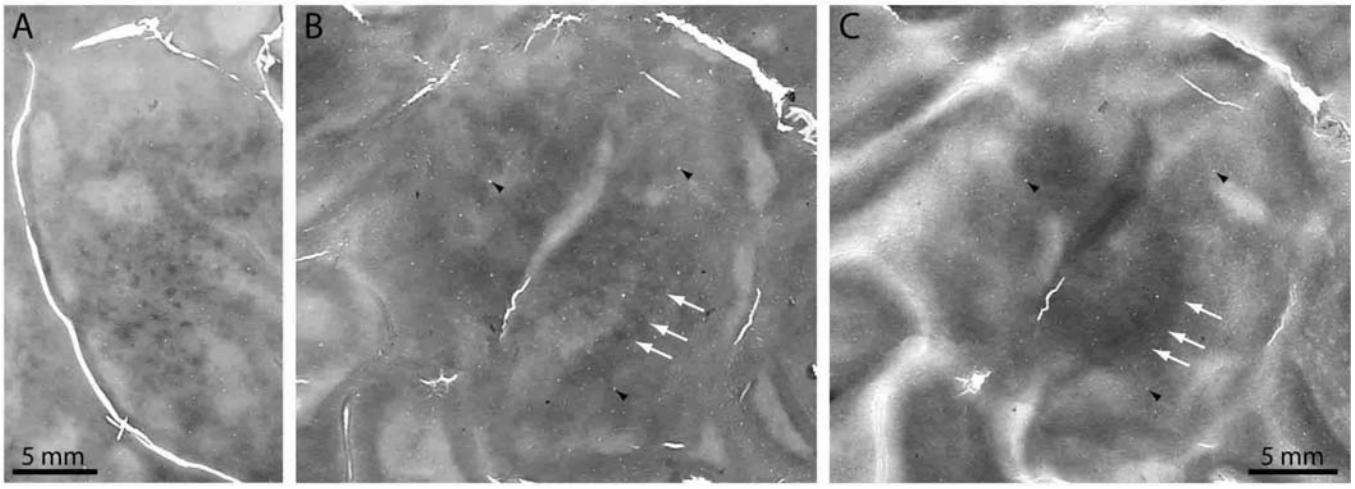

Fig. 14. A: Monkey 5. Region in Fig. 9B, from the superior temporal sulcus, showing CO staining in the vicinity of area MT. In this animal, it consists of a fine pattern of dots, aligned roughly into a grid of 6 x 8 rows, with fluctuation in the background density. B: Monkey 7: In this animal, the CO activity in area MT has a more stripe-like pattern. Arrows mark dark stripes. C: An adjacent section stained with the Gallyas method, showing pale myelin stripes, that are marked by arrows placed in identical locations in B and C. The pale myelin stripes correspond to the dark CO stripes. Arrowheads indicate vessel profiles used for alignment.

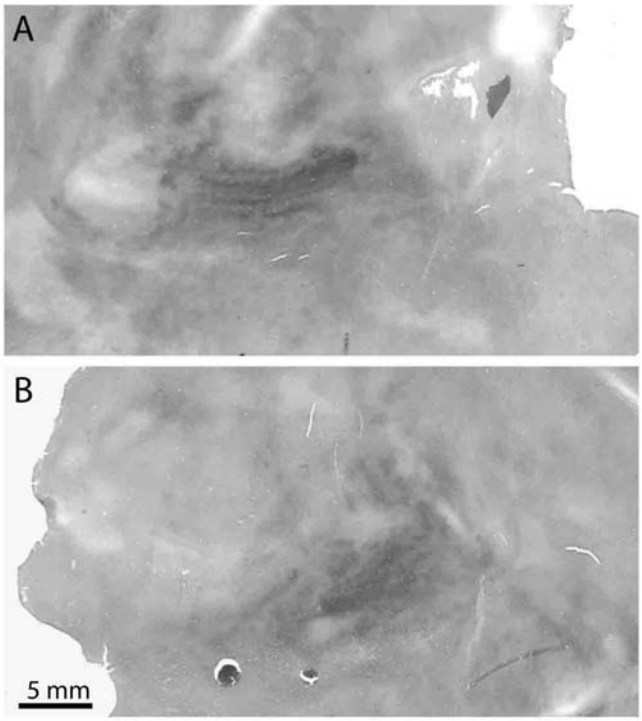

Fig. 15. A: Monkey 6. CO pattern in the right Sylvian fissure corresponding to primary auditory cortex. B: Monkey 1. CO staining in the left Sylvian fissure showing another example of the CO pattern in A1.

identify reliably the cortical layer. However, in other cortical regions, laminar differences in CO activity are nebulous. Moreover, there is always a danger of confusing layer transitions within a single area with cortical boundaries between different areas.

One solution is to extrapolate the relative distance from pial surface or white matter by multiplying the section number and thickness. This is an imperfect approach, because flatmounts are not perfectly flat, so layer transitions within single sections are common. In addition, cortical layers vary in relative thickness in different cortical areas. With these caveats in mind, we used section depth as the main criterion to assign cell labeling to cortical layer in our analysis of the projections to V2 (Fig. 18). We confirmed that the strongest feedback projections arise from the superficial layers and the deep layers (Rockland & Pandya, 1979). However, in certain strongly projecting regions, for example, MT, "V4," and "TEO," the feedback arose from every layer. This was confirmed by examining a given field of labeled cells, section by section, using radially oriented blood vessels as a guide. Labeled cells were found in every single section, from layer 6 (section #14) to layer 2 (section #3). Anderson and Martin (2002) have also observed labeled neurons in layer 4 of MT after tracer injection into V2. We conclude that in many instances, so-called "feedback" projections originate from all layers of cortex, not just superficial and deep layers. This makes it less reliable to use the laminar pattern of retrograde labeling to differentiate between "feedforward" and "feedback" projections (Felleman & Van Essen, 1991).

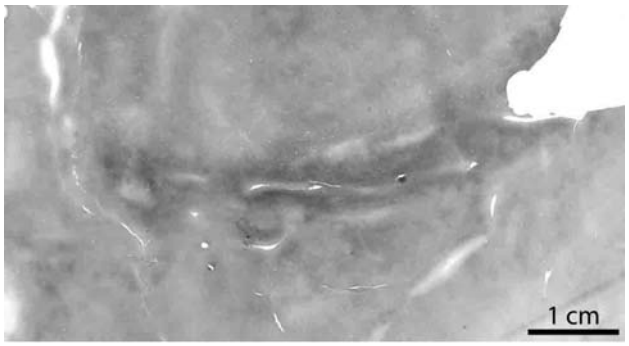

Fig. 16. Monkey 2. Pattern of CO activity in somatosensory cortex of the right hemisphere, in areas 3a, 3b, and 1. For orientation, see raw flatmount in Fig. 4, step 10.

The preparation of a flatmount is more than a simple unfolding of tissue. The cortex has intrinsic curvature which is eliminated by flattening. This process introduces many distortions: in area, shape, distance, direction, and contiguity. It is revealing to see how our physical flatmount and a computer-generated flatmount have distorted the cortex differently (compare Figs. 6 & 8). In computer flatmounts, average absolute areal distortion is reported to range between 16-25%, a figure based on partial cortex reconstructions that omit V1 (Drury et al., 1996).

In physical flatmounts, distortion is hard to measure accurately, but some impression can be gained by comparing familiar regions flattened by different techniques. When striate cortex is isolated and flattened as a single oval piece of tissue (Fig. 9A), the vertical meridian representation is longer than the horizontal meridian representation, because it runs around the outside of V1. We have measured the length of the prime meridia in 12 striate cortices (mean area 1072 mm^2, range 931-1178 mm^2), each flatmounted as a single oval (Horton & Hocking, 1996). The lower vertical meridian was 50.1 mm, the upper vertical meridian was 50.5 mm (mean vertical meridian length = 50.3 mm), and the horizontal meridian was 44.2 mm. The ratio of vertical meridian to horizontal meridian was 1.14:1. In contrast, when striate cortex is split down the middle, the horizontal meridian becomes longer than the vertical meridian, because it now runs on the outside of the specimen. In Fig. 6, the vertical meridian is 54.3 mm and the horizontal meridian is 76 mm, for a ratio of 0.71:1. One can appreciate that switching the V1 relieving cut from the vertical meridian to the horizontal meridian has a huge effect. It increases the relative length of the horizontal meridian and probably increases the overall size of V1, by stretching. The same phenomenon is evident in the computer-generated flatmount. In Fig. 8, the V1 vertical meridia average 61 mm and the horizontal meridian equals 85 mm, for a ratio of 0.72:1. In real life, of course, the cortex has a complex, three-dimensional shape, and the vertical and horizontal meridian may actually be equal in length (Rovamo & Virsu, 1984). These points are pertinent to theories that have argued that ocular dominance columns are oriented perpendicular to the vertical meridian because the vertical meridian is longer than the horizontal meridian.

Another example of the distortion created by flatmounting is provided by the shapes of dorsal and ventral V2. When V1 is flatmounted as an isolated piece, the upper and lower vertical meridian (V1/V2 border) have a perfectly symmetric contour. However, when V1 is split along the horizontal meridian and kept attached to the rest of the hemisphere, the ventral V1/V2 border assumes a more curved configuration. V2 itself becomes thicker and more bowed ventrally, compared to dorsally. This distortion is

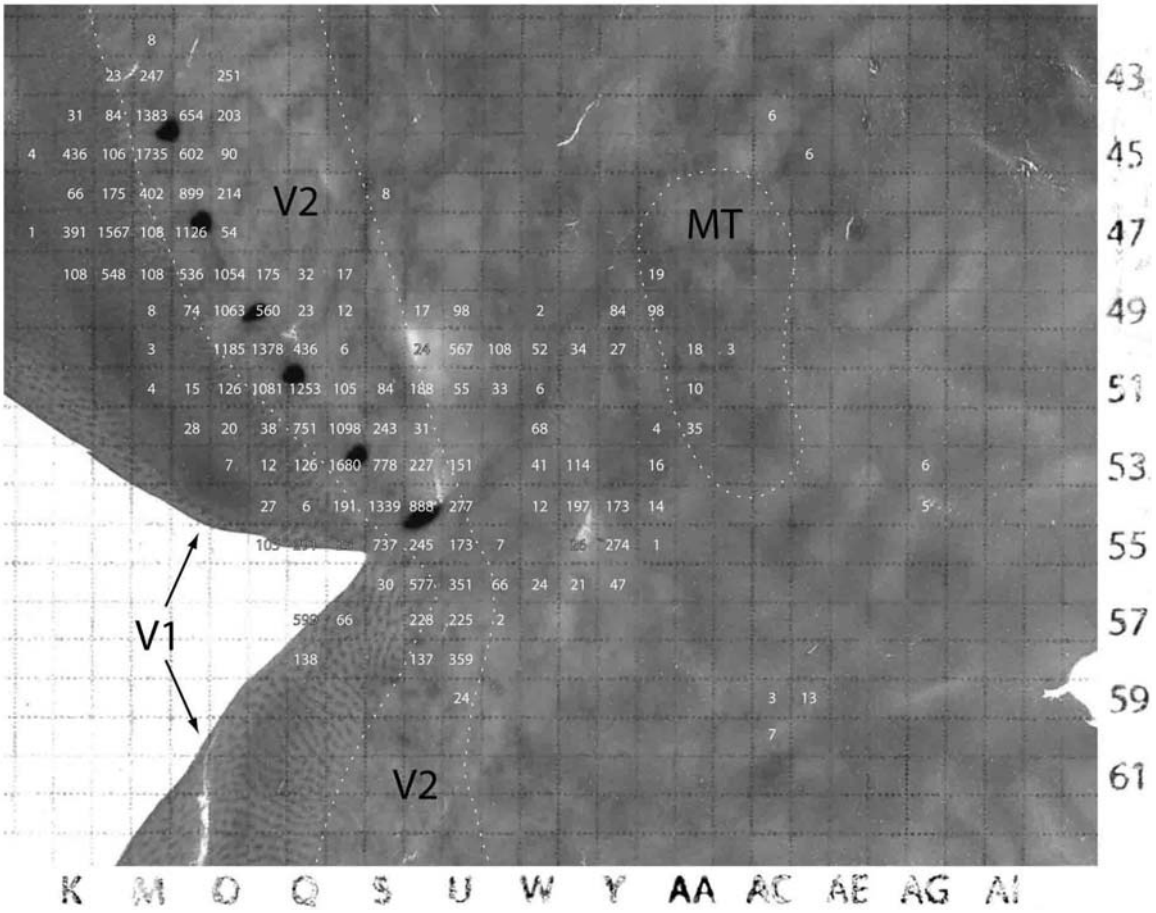

Fig. 17. Monkey 1. Portion of section #7, double labeled for CO and CTB, showing six injection sites in V2, near the border with V1. The grid pattern was printed on the underside of the glass slide. The numbers indicate the quantity of retrogradely labeled cells in each box. The row (K-AI) and column (43-61) labels were moved from their location at the edge of the slide for illustration purposes. The boundaries of V1, V2, and MT (approximate) are shown with dashed lines. Scale: each box is 2 x 2 mm.

due to the overall shape of the flatmount, that is, ventral V2 is contiguous with the temporal lobe, which has a tightly curved perimeter. One could easily eliminate the crescent shape of ventral V2 by extending the third relieving cut (6,6', Fig. 1, step 6) into the occipitotemporal sulcus, rather than towards the superior temporal sulcus, but at the cost of a less compact flatmount and greater distortion elsewhere.

The difference in the shapes of dorsal and ventral V2 in flatmounts was also observed by Olavarria and Van Essen (1997). They felt it was unlikely to be caused by distortion from flattening and proposed that dorso-ventral asymmetry in V2 stripe geometry should be added to the list of differences between regions of cortex associated with lower versus upper visual fields. A striking difference in the shape of dorsal and ventral V2 is also visible in Van Essen's computer-generated flatmounts, but is not reflected in accompanying gray-level maps of areal distortion (Drury et al., 1996; Lewis & Van Essen, 2000). Clearly, recognizing and quantifying distortion is a difficult issue that merits further study. In the case of physical flatmounts, one can take some comfort in a crucial empiric factor: if one attempts to distort the tissue excessively, it simply creates its own relieving cut by tearing. However, lightly fixed cortex is distensible, and we have no quantitative measure of how much stretching can occur before this happens.

With the advent of functional brain mapping, noninvasive imaging has played an increasingly important role in neuroanatomy. The development of computer-based techniques for generating flattened cortex has been useful for depicting the location of cerebral activity. It is not clear, however, that noninvasive imaging can accomplish the goal of mapping the boundaries and connections of the cerebral cortex, because of inherent limitations in resolution. This task will still depend, to a great extent, on preparation of histological sections. Flatmounts allow efficient, direct examination of wide areas of tissue, maintain the physical integrity and spatial relationships of the cortex, and preserve patterns of functional architecture that are often helpful for recognizing areal boundaries. Despite much progress, current maps of the cerebral cortex are still largely a matter of conjecture. As noted by Felleman and Van Essen (1991), among dozens of suggested visual areas, only the boundaries (and identities) of V1, V2, MT, and V3 are known with any real precision. To denote this uncertainty, we have put quotation marks around the names of all visual areas mentioned in this paper, except V1, V2, and MT. We expect that the concerted application of a variety of techniques, including cortical flatmounting, will help reduce this uncertainty in the future.

Starting with a rat cortex sandwiched between two glass slides, the art of flatmounting has progressed incrementally over nearly

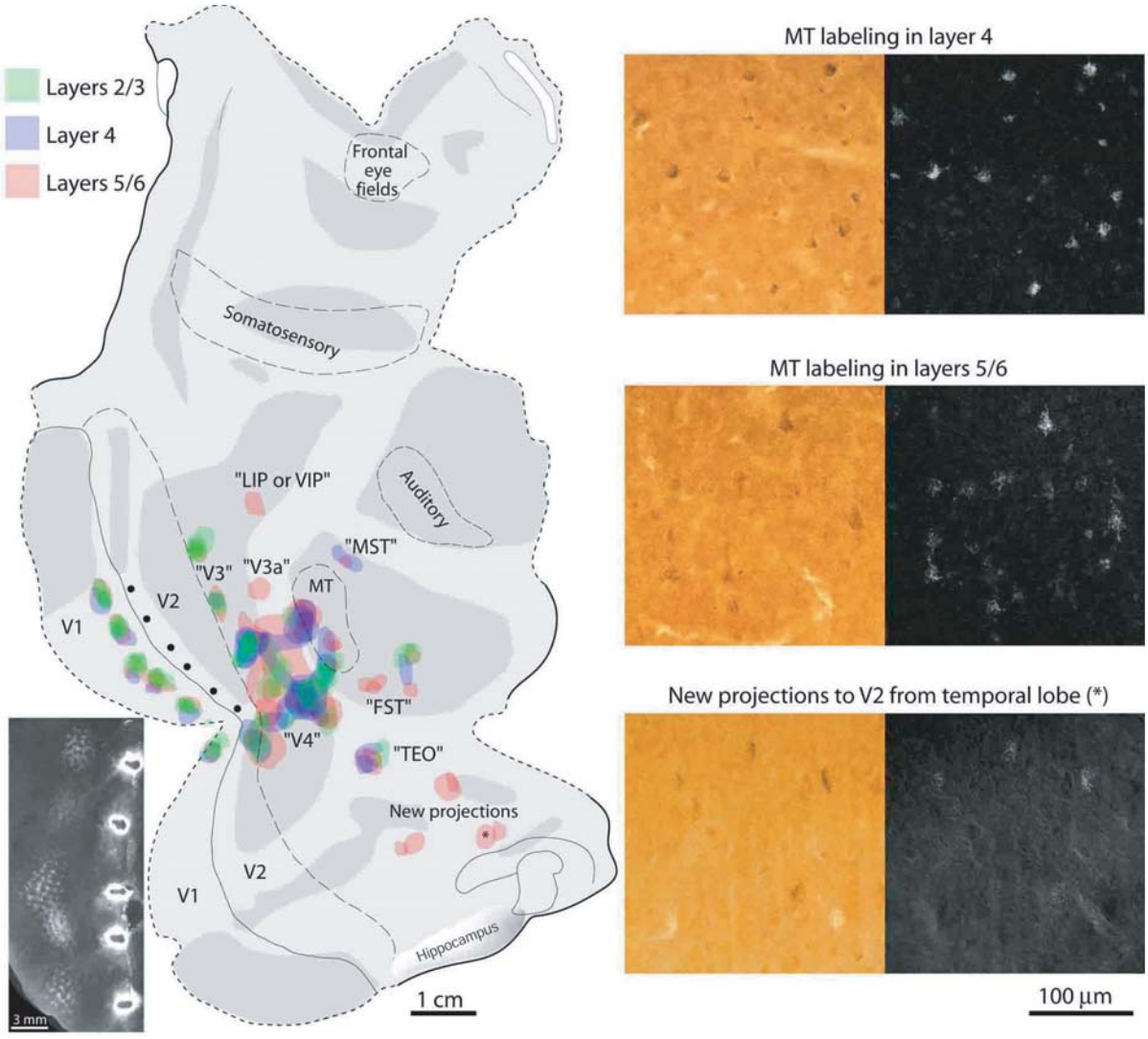

Fig. 18. Monkey 1. Flatmount showing the distribution of labeled cells in layers 2⁄3 (sections 2, 3, 4, 5, 6), layer 4 (sections 7, 8, 9), and layers 5/6 (sections 10, 12, 14) from the six CTB tracer injections in V2 (black dots). Cell labeling in dorsal V2 is not shown. Colored patches denote areas containing retrogradely labeled cells. The abbreviations in quotation marks refer to names of putative visual areas. Darker color saturation indicates that cells were found in more than one section, but otherwise this diagram provides no information about relative cell labeling density. In general, strongest feedback was from layers 5/6, but some strongly labeled regions (e.g. V4, MT) provided feedback from every layer. Examples of labeled cells viewed in lightfield or darkfield with crossed polarizers are shown to the right.

three decades. Curiously, the idea of preparing cortical tissue by stripping away the white matter from the gray matter to aid anatomical studies was first put forward in the 16th Century (Piccolomini, 1586). Having prepared a flatmount of the entire macaque cerebral cortex, the next challenge is to attempt the human cerebral cortex. Although it is much larger in surface area than the macaque's (Fig. 19), there is no technical reason why it cannot be flatmounted successfully.

Acknowledgments

This work was supported by grants R01-EY10217 (J.C.H.) and F32-EY13676 (L.C.S.) from the National Eye Institute. The Beckman Vision Center is supported by core grant P30-EY02162 from the National Eye Institute. Support was also received from Larry L. Hillblom Foundation, That Man May See, Research to Prevent Blindness, and the Bunter Fund. We thank the California Regional Primate Research Center, supported by NIH0NCRR Grant #RR00169, for supplying animals used in this study. Macaque hemispheres were also donated by Stephen Lisberger and Nicholas Priebe. We are grateful to Davina Hocking for her contributions to the flatmount technique and for her artistic drawings. Gloria Choi also provided technical assistance. Melville Wohlgemuth and David Van Essen provided helpful comments on the manuscript.

References

Adams, D.L. & Horton, J.C. (2003). Capricious expression of cortical columns in the primate brain. *Nature Neuroscience* **6**, 113-114.

Allman, J.M. & Kaas, J.H. (1971). A representation of the visual field in the caudal third of the middle temporal gyrus of the owl monkey (Aotus trivirgatus). *Brain Research* **31**, 85-105.

Allman, J.M. & Kaas, J.H. (1974). The organization of the second visual area (V II) in the owl monkey: A second order transformation of the visual hemifield. *Brain Research* **76**, 247-265.

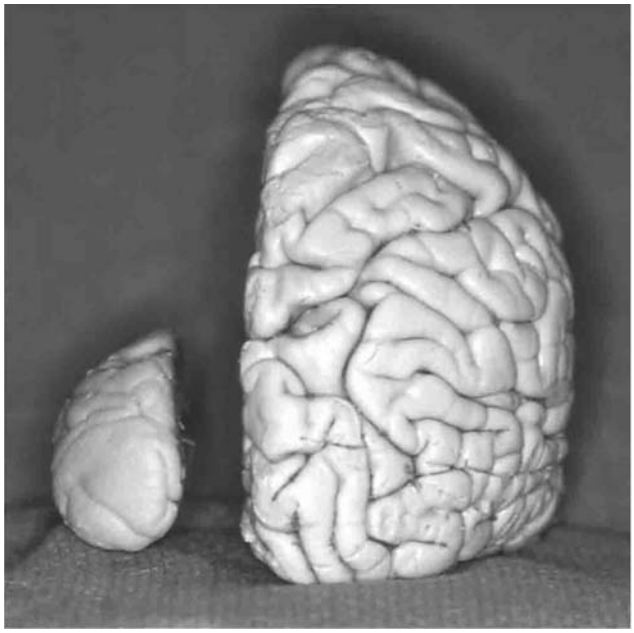

Fig. 19. Comparison of the human and macaque hemispheres (posterior view), photographed together after fixation by immersion in 10% formalin. The human cerebral cortex has about 12-15 times the surface area of the macaque cerebral cortex, but can be flatmounted by following the same general approach outlined in this paper for the macaque.

Allman, J.M. & Kaas, J.H. (1975). The dorsomedial cortical visual area: A third tier area in the occipital lobe of the owl monkey (Aotus trivirgatus). *Brain Research* **100**, 473-487.

Anderson, J.C. & Martin, K.A.C. (2002). Connection from cortical area V2 to MT in macaque monkey. *Journal of Comparative Neurology* **443**, 56-70.

Andrews, T.J., Halpern, S.D. & Purves, D. (1997). Correlated size variations in human visual cortex, lateral geniculate nucleus, and optic tract. *Journal of Neuroscience* **17**, 2859-2868.

Beck, P.D. & Kaas, J.H. (1998). Cortical connections of the dorsomedial visual area in new world owl monkeys (Aotus trivirgatus) and squirrel monkeys (Saimiri sciureus). *Journal of Comparative Neurology* **400**, 18-34.

Beck, P.D. & Kaas, J.H. (1999). Cortical connections of the dorsomedial visual area in old world macaque monkeys. *Journal of Comparative Neurology* **406**, 487-502.

Boyd, J.D. & Casagrande, V.A. (1999). Relationships between cytochrome oxidase (CO) blobs in primate primary visual cortex (V1) and the distribution of neurons projecting to the middle temporal area (MT). *Journal of Comparative Neurology* **409**, 573-591.

Brewer, A.A., Press, W.A., Logothetis, N.K. & Wandell, B.A. (2002). Visual areas in macaque cortex measured using functional magnetic resonance imaging. *Journal of Neuroscience* **22**, 10416-10426.

Brodmann, K. (1909). Vergleichende Lokalisationslehre der Grosshirnrinde in ihren Prinzipien dargestellt auf Grund des Zellenbaues. Leipzig: J. A. Barth.

Brodmann, K. (1918). Individuelle Variationen der Sehsphäre und ihr Bedeutung für die Klinik der Hinterhauptschüsse. *Allgz Psychiat (Berlin)* **74**, 564-568.

Clarke, S. & Rivier, F. (1998). Compartments within human primary auditory cortex: Evidence from cytochrome oxidase and acetylcholinesterase staining. *European Journal of Neuroscience* **10**, 741-745.

Collins, C.E., Stepniewska, I. & Kaas, J.H. (2001). Topographic patterns of V2 cortical connections in a prosimian primate (Galago garnetti). *Journal of Comparative Neurology* **431**, 155-167.

Dale, A.M., Fischl, B. & Sereno, M.I. (1999). Cortical surface-based analysis. I. Segmentation and surface reconstruction. *Neuroimage* **9**, 179-194.

Desimone, R. & Ungerleider, L.G. (1986). Multiple visual areas in the caudal superior temporal sulcus of the macaque. *Journal of Comparative Neurology* **248**, 164-189.

De Vries, I. (1912). Über die Zytoarchitektonik der Grosshirnrinde der Maus und über die Beziehungen der einzelnen Zellschichten zum Corpus Callosum auf Grund von experimentellen Läsionen. *Folia neuro-biol* **6**, 288-322.

DeYoe, E.A. & Van Essen, D.C. (1985). Segregation of efferent connections and receptive field properties in visual area V2 of the macaque. *Nature* **317**, 58-61.

Droogleever Fortuyn, A.B. (1914). Cortical cell-lamination of the hemispheres of some rodents. *Archives of Neurology and Psychiatry (Mott's)* **6**, 221-354.

Drury, H.A., Van Essen, D.C., Anderson, C.H., Lee, C.W., Coogan, T.A. & Lewis, J.W. (1996). Computerized mappings of the cerebral cortex: A multiresolution flattening method and a surface-based coordinate system. *Journal of Cognitive Neuroscience* **8**, 1-28.

Eskenasy, A.C. & Clarke, S. (2000). Hierarchy within human SI: Supporting data from cytochrome oxidase, acetylcholinesterase and NADPH-diaphorase staining patterns. *Somatosensory and Motor Research* **17**, 123-132.

Felleman, D.J. & Van Essen, D.C. (1991). Distributed hierarchical processing in the primate cerebral cortex. *Cerebral Cortex* **1**, 1-47.

Felleman, D.J., Xiao, Y. & McClendon, E. (1997). Modular organization of occipito-temporal pathways: Cortical connections between visual area 4 and visual area 2 and posterior inferotemporal ventral area in macaque monkeys. *Journal of Neuroscience* **17**, 3185-3200.

Fischl, B., Sereno, M.I. & Dale, A.M. (1999). Cortical surface-based analysis. II: Inflation, flattening, and a surface-based coordinate system. *Neuroimage* **9**, 195-207.

Gallyas, F. (1979). Silver staining of myelin by means of physical development. *Neurological Research* **1**, 203-209.

Gattass, R. & Gross, C.G. (1981). Visual topography of striate projection zone (MT) in posterior superior temporal sulcus of the macaque. *Journal of Neurophysiology* **46**, 621-638.

Gattass, R., Sousa, A.P., Mishkin, M. & Ungerleider, L.G. (1997). Cortical projections of area V2 in the macaque. *Cerebral Cortex* **7**, 110-129.

Horton, J.C. (1984). Cytochrome oxidase patches: A new cytoarchitectonic feature of monkey visual cortex. *Philosophical Transactions of the Royal Society B* (London) **304**, 199-253.

Horton, J.C. & Hocking, D.R. (1996). Intrinsic variability of ocular dominance column periodicity in normal macaque monkeys. *Journal of Neuroscience* **16**, 7228-7239.

Horton, J.C. & Hocking, D.R. (1997). Myelin patterns in V1 and V2 of normal and monocularly enucleated monkeys. *Cerebral Cortex* **7**, 166-177.

Horton, J.C. & Hubel, D.H. (1981). Regular patchy distribution of cytochrome oxidase staining in primary visual cortex of macaque monkey. *Nature* **292**, 762-764.

Hubel, D.H. & Wiesel, T.N. (1969). Anatomical demonstration of columns in the monkey striate cortex. *Nature* **221**, 747-750.

Jones, E.G., Dell'Anna, M.E., Molinari, M., Rausell, E. & Hashikawa, T. (1995). Subdivisions of macaque monkey auditory cortex revealed by calcium-binding protein immunoreactivity. *Journal of Comparative Neurology* **362**, 153-170.

Jones, E.G., Woods, T.M. & Manger, P.R. (2002). Adaptive responses of monkey somatosensory cortex to peripheral and central deafferentation. *Neuroscience* **111**, 775-797.

Kennedy, H. & Bullier, J. (1985). A double-labeling investigation of the afferent connectivity to cortical areas V1 and V2 of the macaque monkey. *Journal of Neuroscience* **5**, 2815-2830.

Krubitzer, L.A. & Kaas, J.H. (1990). Cortical connections of MT in four species of primates: Areal, modular, and retinotopic patterns. *Visual Neuroscience* **5**, 165-204.

Krubitzer, L.A. & Kaas, J.H. (1993). The dorsomedial visual area of owl monkeys: Connections, myeloarchitecture, and homologies in other primates. *Journal of Comparative Neurology* **334**, 497-528.

LeVay, S., Connolly, M., Houde, J. & Van Essen, D.C. (1985). The complete pattern of ocular dominance stripes in the striate cortex and visual field of the macaque monkey. *Journal of Neuroscience* **5**, 486-501.

Lewis, J.W. & Van Essen, D.C. (2000). Mapping of architectonic subdivisions in the macaque monkey, with emphasis on parieto-occipital cortex. *Journal of Comparative Neurology* **428**, 79-111.

Livingstone, M.S. & Hubel, D.H. (1984). Anatomy and physiology of a color system in the primate visual cortex. *Journal of Neuroscience* **4**, 309-356.

Llewellyn-Smith, I.J., Minson, J.B., Wright, A.P. & Hodgson, A.J. (1990). Cholera toxin B-gold, a retrograde tracer that can be used in light and electron microscopic immunocytochemical studies. *Journal of Comparative Neurology* **294**, 179-191.

Lorente De Nó, R. (1922). La corteza cerebral del ratón. *Trabajos del Laboratorio de Investigaciones Biológicas de la Universidad de Madrid* **20**, 41-78.

Lyon, D.C. & Kaas, J.H. (2001). Connectional and architectonic evidence for dorsal and ventral V3, and dorsomedial area in marmoset monkeys. *Journal of Neuroscience* **21**, 249-261.

Lyon, D.C. & Kaas, J.H. (2002). Evidence for a modified v3 with dorsal and ventral halves in macaque monkeys. *Neuron* **33**, 453-461.

Maunsell, J.H.R. & Van Essen, D.C. (1987). Topographic organization of the middle temporal visual area in the macaque monkey: Representational biases and the relationship to callosal connections and myeloarchitectonic boundaries. *Journal of Comparative Neurology* **266**, 535-555.

Mouritzen Dam, A. (1979). Shrinkage of the brain during histological procedures with fixation in formaldehyde solutions of different concentrations. *Journal of Hirnforsch* **20**, 115-119.

Olavarria, J.F. & Van Sluyters, R.C. (1985). Unfolding and flattening the cortex of gyrencephalic brains. *Journal of Neuroscience Methods* **15**, 191-202.

Olavarria, J.F. & Van Essen, D.C. (1997). The global pattern of cytochrome oxidase stripes in visual area V2 of the macaque monkey. *Cerebral Cortex* **7**, 395-404.

Penfield, W. & Boldrey, E. (1937). Somatic motor and sensory representation in the cerebral cortex of man as studied by electrical stimulation. *Brain* **60**, 389-443.

Piccolomini, A. (1586). *Anatomicae praelectiones explicantes mirificam corporis humani fabricam* (Rome). Translated in E. Clarke and C.D. O'Malley, *The Human Brain and Spinal Cord*, San Francisco: Norman Publishing, pp. 387-388.

Preuss, T.M., Beck, P.D. & Kaas, J.H. (1993). Areal, modular, and connectional organization of visual cortex in a prosimian primate, the slow loris (Nycticebus coucang). *Brain, Behavior and Evolution* **42**, 321-335.

Rockland, K.S. & Pandya, D.N. (1979). Laminar origins and terminations of cortical connections of the occipital lobe in the rhesus monkey. *Brain Research* **179**, 3-20.

Rockland, K.S. & Van Hoesen, G.W. (1994). Direct temporal-occipital feedback connections to striate cortex (V1) in the macaque monkey. *Cerebral Cortex* **4**, 300-313.

Roe, A.W. & Ts'o, D.Y. (1999). Specificity of color connectivity between primate V1 and V2. *Journal of Neurophysiology* **82**, 2719-2730.

Rose, M. (1912). Histologische Lokalisation der Grosshirnrinde bei kleinen Säugetieren (Rodentia, Insectivora, Chiroptera). *Journal für Psychologie und Neurologie (Leipzig)* **19**, 389-479.

Rovamo, J. & Virsu, V. (1984). Isotropy of cortical magnification and topography of striate cortex. *Vision Research* **24**, 283-286.

Sereno, M.I., Dale, A.M., Reppas, J.B., Kwong, K.K., Belliveau, J.W., Brady, T.J., Rosen, B.R. & Tootell, R.B. (1995). Borders of multiple visual areas in humans revealed by functional magnetic resonance imaging. *Science* **268**, 889-893.

Sherk, H. (1992). Flattening the cerebral cortex by computer. *Journal of Neuroscience Methods* **41**, 255-267.

Sincich, L.C. & Horton, J.C. (2002a). Divided by cytochrome oxidase: A map of the projections from V1 to V2 in macaques. *Science* **295**, 1734-1737.

Sincich, L.C. & Horton, J.C. (2002b). Pale cytochrome oxidase stripes in V2 receive the richest projection from macaque striate cortex. *Journal of Comparative Neurology* **447**, 18-33.

Stensaas, S.S., Eddington, D.K. & Dobelle, W.H. (1974). The topography and variability of the primary visual cortex in man. *Journal of Neurosurgery* **40**, 747-755.

Stepniewska, I. & Kaas, J.H. (1996). Topographic patterns of V2 cortical connections in macaque monkeys. *Journal of Comparative Neurology* **371**, 129-152.

Tootell, R.B. & Silverman, M.S. (1985). Two methods for flat-mounting cortical tissue. *Journal of Neuroscience Methods* **15**, 177-190.

Tootell, R.B., Silverman, M.S., Switkes, E. & De Valois, R.L. (1982). Deoxyglucose analysis of retinotopic organization in primate striate cortex. *Science* **218**, 902-904.

Tootell, R.B., Hamilton, S.L. & Silverman, M.S. (1985). Topography of cytochrome oxidase activity in owl monkey cortex. *Journal of Neuroscience* **5**, 2786-2800.

Tootell, R.B.H. & Taylor, J.B. (1995). Anatomical evidence for MT and additional cortical visual areas in humans. *Cerebral Cortex* **1**, 39-55.

Tootell, R.B.H., Silverman, M.S., De Valois, R.L. & Jacobs, G.H. (1983). Functional organization of the second cortical visual area in primates. *Science* **220**, 737-739.

Van Essen, D.C. (2003). Organization of visual areas in macaque and human cerebral cortex. In *Visual Neurosciences*, ed. Werner, J.S. & Chalupa, L.M., pp. 507-522. Cambridge, Massachusetts: MIT Press.

Van Essen, D.C. & Zeki, S.M. (1978). The topographic organization of rhesus monkey prestriate cortex. *Journal of Physiology* **277**, 193-226.

Van Essen, D.C. & Maunsell, J.H.R. (1980). Two-dimensional maps of the cerebral cortex. *Journal of Comparative Neurology* **191**, 255-281.

Van Essen, D.C., Maunsell, J.H.R. & Bixby, J.L. (1981). The middle temporal visual area in the macaque: myeloarchitecture, connections, functional properties and topographic organization. *Journal of Comparative Neurology* **199**, 293-326.

Van Essen, D.C., Newsome, W.T. & Maunsell, J.H. (1984). The visual field representation in striate cortex of the macaque monkey: Asymmetries, anisotropies, and individual variability. *Vision Research* **24**, 429-448.

Van Essen, D.C., Lewis, J.W., Drury, H.A., Hadjikhani, N., Tootell, R.B., Bakircioglu, M. & Miller, M.I. (2001). Mapping visual cortex in monkeys and humans using surface-based atlases. *Vision Research* **41**, 1359-1378.

Welker, C. & Woolsey, T.A. (1974). Structure of layer IV in the somatosensory neocortex of the rat: Description and comparison with the mouse. *Journal of Comparative Neurology* **158**, 437-453.

Wong-Riley, M. & Carroll, E.W. (1984). Effect of impulse blockage on cytochrome oxidase activity in monkey visual system. *Nature* **307**, 262-264.

Woolsey, T.A. & Van Der Loos, H. (1970). The structural organization of layer IV in the somatosensory region (S1) of mouse cerebral cortex: The description of a cortical field composed of cytoarchitectonic units. *Brain Research* **17**, 205-242.

Zeki, S.M. (1978). The third visual complex of rhesus monkey prestriate cortex. *Journal of Physiology* **277**, 245-272.